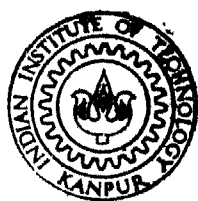


**FINITE ELEMENT ANALYSIS OF NON-LINEAR HEAT
CONDUCTION THROUGH CONTINUOUS-FIBER-
REINFORCED COMPOSITES**

By
V. SOMASUNDARAM



**DEPARTMENT OF MECHANICAL ENGINEERING
IN INSTITUTE OF TECHNOLOGY, KANPUR
MARCH, 1984**

10 JUL 1984

83400

ME-1904-M-SEM-FIN

CERTIFICATE

7/3/84
R.S.

This is to certify that this work on "Finite Element Analysis of Non-Linear Heat Conduction Through Continuous-Fiber-Reinforced Composites" has been carried out under my supervision and has not been submitted elsewhere for a Degree.

MARCH, 1984

Dr. C. C. Agarwal
(H. C. AGRAWAL)
PROFESSOR
DEPARTMENT OF MECHANICAL ENGINEERING
INDIAN INSTITUTE OF TECHNOLOGY
KANPUR

POST GRADUATE OFFICE

This thesis has been approved
for the award of the Degree of
Master of Technology (M.Tech.)
in accordance with the
regulations of the Indian
Institute of Technology, Kanpur

1984 27/3/84

ACKNOWLEDGEMENT

At the very outset, I wish to express my indebtedness to Prof. H.C. Agrawal, who initiated discussions that led to the present work, for his guiding spirit and encouragement.

I would also like to utilize this opportunity to accord special gratitude to Shri M.K. Patra, a brilliant scholar in the department of Aeronautical Engineering, without whose help, perhaps, this work could not have attained its present form.

Further, thanks are due to Shri D.P. Saini for his elegant typing and the rest of the staff and faculty of Mechanical Engineering.

Words fail me, however, when I wish to express the amount of support I have received from my colleagues and circle of friends. I am forever, obliged to them.

Lest I forget, I am greatly indebted to my parents and family for their patience and forbearance.

V. SOMASUNDARAM

NOMENCLATURE

Greek Symbols:

α	= 1 for Fiber
α	= 2 for Matrix
δt	= Small time interval
δT	= Small temperature difference
η_1, η_2, η_3	= Natural coordinates for the triangular finite element
Θ	= Angular coordinate
\emptyset	= Field variable
μ	= Specific heat per unit volume

Alphabetical Symbols:

A	= Area of the 2-D finite element
B_1, B_2, B_3	= Constants
C_1, C_2, C_3	= Constants
D	= Domain of the finite element
f	= See table 2.1
$[F]$	= Heat flux matrix
g	= See table 2.1
h	= See table 2.1
K	= Thermal conductivity
K_x, K_y, K_z	= See table 2.1
$[K]$	= Thermal stiffness matrix
N_i	= Interpolating function
r	= Radial coordinate

r_1 = Radius of fiber
 r_2 = Radius of equivalent cell
 s_1, s_2 = Domain boundary segments
 T = Temperature
 T_0 = Applied temperature
 t = Time
 t_0 = Impulse duration
 x = Axial coordinate

Superscripts:

$\alpha, (\alpha)$ = α - constituent
 (e) = Finite element (e)

Subscripts:

1 = Fiber
 2 = Matrix
 x = In the axial direction
 r = In the radial direction
 i, j, k = Nodes of triangular finite element.

ABSTRACT

A formulation has been developed to study the phenomenon of one-dimensional Heat Conduction through Unidirectional, Continuous Fiber Reinforced Composites. Further, a transient Finite Element procedure has been developed to solve the above formulation for variations in thermal properties and composite geometries.

An initial boundary value problem has been selected and solved for temperature-dependent thermal properties. System sensitivity to non-linearities arising from temperature dependence of thermal properties has been examined extensively for composites having a constant Fiber-Matrix volume fraction.

The Finite Element Method results have been presented in the graphical form and discussed. It has been found and demonstrated that non-linear behaviour of thermal properties could significantly alter system responses.

CONTENTS

		<u>Page No.</u>
CERTIFICATE		
ACKNOWLEDGEMENT		
NOMENCLATURE		
ABSTRACT		
CHAPTER 1	: INTRODUCTION	1
1.1	: Composite Materials	1
1.1.1	: Characteristics	1
1.1.2	: Classification	2
1.1.3	: Fibrous Composites	4
1.1.4	: Fibrous Composites as insulators	5
1.1.5	: Heat Diffusion in Fiber Reinforced Composites	6
1.2	: Finite Element Method in Thermal Analysis	7
1.2.1	: Essence of the method	8
1.3	: Preview of past work The present work	12
CHAPTER 2	:	
2.1	: The field problem	17
2.2	: Formulation	19
2.2.1	: Composition	19
2.2.2	: Geometry	21
2.2.3	: Formulation	21

2.3	: Finite Element formulation	25
2.3.1	: Finite Element discretization	27
2.3.2	: General matrix equations	37
2.4	: Solution package	39
CHAPTER 3		
3.1	: Results and discussions	43
3.2	: Conclusions	48
REFERENCES		57

LIST OF FIGURES

	<u>PAGE</u>
1.1	Classification of composite materials
1.2	Problem domain, boundary and elements
2.1	3-D Solution domain
2.2	Hexagonal array-composite cylinder construction
2.3	Geometry and coordinate system
2.4	Symmetrical half cross section and boundary conditions
2.5	Triangular ring element
2.6	Section and coordinates of ring element (Triangular)
2.7	Finite element mesh for analysis
3.1	Average axial temperature distribution before withdrawal of temperature source (Graphite/Epoxy)
3.2	Average axial temperature distribution after withdrawal of temperature source (Graphite/Epoxy)
3.3	Temperature-time history at an intermediate region (Graphite/Epoxy)
3.4	Radial temperature distribution before and after withdrawal of temperature source (Graphite/Epoxy)
3.5	Average axial temperature distribution before removal of temperature source (Carbon/Carbon)
3.6	Average axial temperature distribution after removal of temperature source (Carbon/Carbon)
3.7	Temperature-time history at an intermediate region (Carbon/Carbon)
3.8	Radial temperature distribution before and after withdrawal of temperature source(Carbon/Carbon)

Chapter 1

INTRODUCTION

1.1 COMPOSITE MATERIALS

A composite material, in general, could be defined, as one having two or more distinct constituent materials or phases. They offer outstanding mechanical properties coupled with flexibility in design and ease of fabrication. The use of composite materials has become quite common, these days, in industries like aircraft, automobile, sports-goods and electronics. Notable among the many composite materials, are the fiber composites which have the ability to make use of the outstanding strength, stiffness and low specific gravity of fibers such as glass, graphite or Kevlar. Also, in the case of fiber composites, the ability to synthesize the material structure during manufacture is a great advantage.

1.1.1 Characteristics

Composites consist of one or more discontinuous phases embedded in a continuous phase called the matrix. The discontinuous phase is usually harder, stronger and

primarily meant for reinforcement. An exception is the class of rubber-modified polymers, which have a rigid polymer matrix filled with rubber particles.

The properties of composite materials are strongly influenced by the properties of their constituents, their distribution and the interaction between them. They also depend on the geometry of the reinforcement with reference to the system. Concentration, measured in terms of volume or weight fraction, is perhaps the parameter with greatest influence on composite properties. It being controllable during manufacture, desired properties of the composite could be created with great facility. The concentration distribution of the particles, which depends on their spatial relations, is a measure of the homogeneity of the system. The orientation of the reinforcement affects the isotropy of the system.

1.1.2 Classification

The strengthening mechanism of a composite, strongly, depends on the geometry of the reinforcement and hence, it would be useful to classify them accordingly.

Composite materials can be, in this light, broadly classified as fibrous composites and particulate composites. Fig. 1.1 gives a more detailed classification.

COMPOSITE MATERIALS

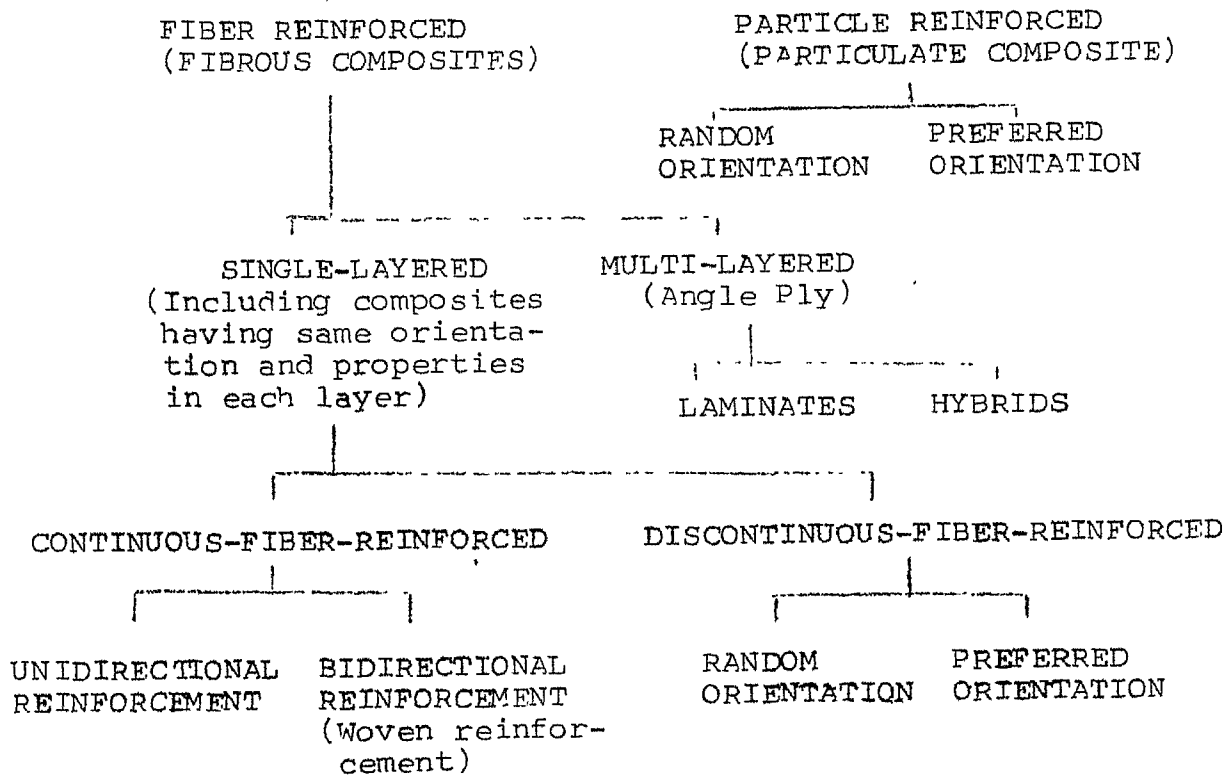


Fig. 1.1

The chief characteristic of a particle is that it is non-fibrous in that, its length is not very much greater than its cross-sectional dimensions. As our study is related to fibrous composites, let us have a more detailed look at their characteristics.

1.1.3 Fibrous Composites

With normal engineering materials, imperfections in a direction normal to applied loads are particularly detrimental to their behaviour. Man-made fibres have considerably lesser flaws perpendicular to their lengths and are therefore, stronger, resulting in their use as reinforcements.

The most important reinforcement fiber is E-glass because of its relatively lower cost. Boron, graphite and aramid polymer fibers (Kevlar 49) are useful for their high stiffness.

Fibers, because of their small cross-sectional dimensions, are not directly utilized in engineering applications but are used as fibrous composites by embedding them in matrix materials. The matrix serves to bind the fibers together, transfer loads to the fibers, and protect them against environmental attack and damage due to handling.

Fibrous composites can be broadly classified as single-layer and multi-layer (angle-ply) composites.

"Single-layer" composites may, actually, be made-up of several distinct layers, each layer having the same orientation and properties. The entire laminate, thus, behaves like a "Single-layer" composite. "Multi-layer" composites, on the other hand, consists of several layers, each layer or lamina being a single-layer composite. The orientation of these single-layers is varied according to the desired design.

When the constituent materials in each layer are the same, they are called laminates. Hybrid laminates are multi-layered composites with layers made up of different materials.

The chief advantages of employing fibrous composites lie in their high strength-to-weight ratio and their controlled anisotropy which facilitates variation in desired ratios of properties in different directions.

1.1.4 Fibrous Composites as Insulators

The combination of high stiffness and strength with low weight enables fibrous composites to be natural candidates for aerospace applications. They are employed in supersonic transport to accommodate thermal stresses,

in space transport as heat shields and nose-tip insulators, and in space structures to reduce thermal deflections.

An outstanding example of their use as insulators is the case of the reusable surface insulation (RSI) tiles employed on the space shuttle orbiter [1]. Their cost effectiveness, resistance to thermal shock and high insulative efficiency make them the best choice for such applications. The RSI tiles consist of silicon fibers dispersed in silicon carbide.

Heat treated polyacrylonitrile (PAN) based carbon felt, in a rough laminar carbon matrix, gives a material with high resistance to thermal shock [2]. PAN-felt carbon, in chemically vapor deposited carbon matrices, also are good insulators [3].

1.1.5 Heat Diffusion in Fiber Reinforced Composites

It has been observed that temperature and moisture are the primary environmental conditions that affect the behaviour of a structural composite during its service life. Hence, the analysis of thermal and/or moisture fields in a composite is of great importance.

Conduction, parallel to the fibers of an unidirectional fibrous composite, is a problem of considerable practical importance for those cases in which such

composites are used as thermal insulators. Re-entry vehicle heat shields and nose-tips, in which the primary direction of heat flow is the fiber axis, are typical examples.

The reduction of these problems to the one dimensional type entails greater computational efficiency. Most materials, used currently for these purposes, exhibit temperature dependent diffusive properties. The resulting nonlinearities render analytical treatment intractable. While considerable work has been carried out on the finite element analysis of conduction, the studies were limited to linear cases [4]. It is, therefore, of interest to analyse the non-linear heat transfer under such circumstances.

1.2 FINITE ELEMENT METHOD IN THERMAL ANALYSIS

The Finite Element Method (FEM) was first applied to structural analysis. The approach is now recognised as applicable to any problem that can be formulated in the differential or variational form. This recognition is a boon to the analysis of thermal fields and coupled problems which arise in many applications. Aerospace structures, specially, can operate in severe thermal environs which significantly affect their structural design. Examples include convectively cooled structures

under development for hypersonic transport, thermal protection systems for the space shuttle and large flexible space structures currently being designed for earth orbit. The design of these systems requires a strong interaction between thermal and structural analyses. The FEM offers the greatest potential for efficient coupling of the two [5].

1.2.1 Essence of the Method

The heat diffusion equation could be written as,

$$\nabla^T K \nabla' T + Q - c \frac{\partial T}{\partial t} = 0 \quad (1.1)$$

which is a classical example of a continuum mathematical problem.

The numerical 'discretization' of such a continuum problem with its boundary conditions

$$T - \bar{T} = 0 \quad \text{on } \omega_1 \quad (1.2)$$

$$n^T k \nabla T - q = 0 \quad \text{on } \omega_2$$

is the essence of all numerical solutions, where ω_1 and ω_2 are portions of the boundary on which temperatures \bar{T} or fluxes q are given and n represents the unit normal vector to the boundary.

The finite element method can, in general, be defined as a process wherein,

(i) the continuous function T is approximated by a series of parameters a_i and specified trial functions $N_i(x,y,z)$ in the problem domain Ω as

$$T \approx \hat{T} = \sum N_i a_i ; \quad i = 1 \dots n \quad (1.3)$$

(ii) writing the differential equation (such as (1.1)) and its boundary conditions (such as (1.2)) in the general form:

$$\begin{aligned} A(T) &= 0 \quad \text{in } \Omega \\ B(T) &= 0 \quad \text{in } \omega \end{aligned} \quad (1.4)$$

The approximating equations, from which the solution is to be obtained, are written as a set

$$\int_{\Omega} w_j A(\hat{T}) d\Omega + \int_{\omega} \bar{w}_j B(\hat{T}) d\omega = 0 \quad j = 1 \dots n \quad (1.5)$$

where w_j and \bar{w}_j are suitable weighting functions which ensure that as $n \rightarrow \infty$

$$\begin{aligned} A(\hat{T}) &\rightarrow 0 \quad \text{in } \Omega \\ \text{and } B(\hat{T}) &\rightarrow 0 \quad \text{in } \omega \end{aligned} \quad (1.6)$$

i.e., at all points, the approximating solution tends to the exact solution.

The definite integral of equation (1.5) can be written as simply a sum of such integrals occurring on 'subdomains' into which the whole 'domain' is divided (Fig. 1.2). Thus, if



Fig.1.2 . PROBLEM DOMAIN, BOUNDARY AND NUMBERS

$$\Omega = \sum_{e=1}^m \Omega^e \text{ and } \omega = \sum_{e=1}^m \omega^e \quad (1.7)$$

then, for all finite functions (), we have,

$$\int_{\Omega} () d\Omega = \sum_{e=1}^m \int_{\Omega^e} () d\Omega \quad (1.8)$$

$$\int_{\omega} () d\omega = \sum_{e=1}^m \int_{\omega^e} () d\omega$$

where, Ω^e and ω^e are associated with 'elements' into which we divide the problem.

This allows the whole region to be divided into standard type of sub-regions, in which the parameters a_i are usually the nodal values of the independent function T and in which the trial functions are defined in a local manner. The integrals can, then, be evaluated element by element and the approximating equations (such as (1.5)) obtained by a simple addition of element contributions.

1.3 PREVIEW OF PAST WORK

On reviewing the work done in the area of conduction, it was found that while literature is rich with various methods for the solution of linear problems, there is relatively little material available on non-linear problems.

In 1951, Storm [6] showed that the mathematical condition for conversion of the 1-D non-linear conduction problem to the linear case is the constancy of $[1/(KS)]^{1/2}$ $\frac{d}{dt} [\log (S/K)]^{1/2}$. The conversion, however, was found valid only for simple metals.

Pattle [7], in 1959, presented a closed form solution to the non-linear problem using an integral method for the restrictive case of an internal heat source in an infinite medium whose thermal conductivity follows some power law $K(T) \sim T^n$. During the same year, Yang et al., [8], discussed the integral method for multicomponent planar solids.

Tsang [9], Andre-Talaman [10] and Olsson [11], in later years, discussed small perturbation methods to solve non-linear conduction problems. However, these methods are complicated to use, as it becomes difficult to obtain solutions to higher order perturbation terms.

Goodman [12] and Imber [13] have described integral or heat balance methods of considerably low accuracy. The latter amended the integral method to include phase change problems.

Padovan [14], in 1974 used complex series representations and properties of adjoint differential operators to develop a finite element procedure for non-linear conduction, which is rather complicated to use.

Leelamma et al., [4], in 1981, have pointed out the non-availability of finite element solutions to non-linear conduction problems, thus far, and proposed a perturbation method for weakly non-linear cases of an isotropic material.

Analysis of behaviour of composite materials began, rather, late. It was only in the early seventies (1971-1973) that some research was carried out on diffusion in composites. Bedford and Stern [15,16] proposed a continuum theory for diffusion in composites, modelling the constituents as superimposed continua. The same theory was found effective for one-dimensional wave propagation in composites in the direction of reinforcement. Hegemier and others [17,18] presented a continuum theory and an analytical procedure for modelling wave propagation in laminated and uni-directional fiber composites.

The theory takes care of mixture interaction and micro-structural information, but is restricted in application to wave propagation only.

Horvay et al., [19], first studied the case of transient heat conduction in laminated composites, omitting the case of fiber composites. Padovan [20] gave an analytical solution for transient temperature distribution of a 2-D general anisotropic half space. Later, using a variational procedure, he developed a finite element approximation for steady heat conduction in anisotropic media [21,22]. The methods, however, are not applicable for transient and non-linear situations.

Haltman et al., [23], examined experimentally and numerically, steady heat conduction in a two phase, two-dimensional model of aluminium bars dispersed in foamed polyurethane. Hegemier et al., [24,25,26], gave various continuum theories related to fiber reinforced composites and laminated composites but, applicable to the phenomenon of wave propagation only. In 1975, Nayfeh [27] gave a continuum mixture theory for heat conduction in laminated wave guides, using approximations enabling analytical solutions.

Chen et al., [28], calculated the thermal conductivity of composite materials containing thinly

dispersed spheroidal inclusions. The associated problems of heat flow across one such inclusion embedded in an infinite matrix were solved, in the presence of thermal boundary resistance. Maewal et al., [29], developed a continuum model for wave propagation problems, and applied it for diffusion type processes also, in a laminated composite with periodic microstructure and obtained finite difference solutions. Again, Maewal et al., [30] and Murakami et al., [31] developed mixture theories for the process of heat transfer in unidirectional fibrous composites with periodic hexagonal microstructure.

Patankar [32], gave a finite difference solution of heat conduction in the case of non-uniform thermal conductivity in a composite slab. Poon [33], reviews the various methods to solve problems of heat conduction in laminated composites. Murakami et al., [34], extended their earlier work [30], to include non-linear material behaviour. Laura [35], gave analytical and numerical solutions to determine the temperature distribution in a composite rod with variable internal heat generation.

It was in April 1983, that Arun Aggarwal [36] developed a Finite Element Analysis package for the longitudinal heat diffusion in fiber-reinforced composites. The work, however did not consider non-linearities arising due to temperature dependent material properties.

The Present Work

In the present work, non-linearities arising due to temperature dependence of material properties have been taken care of as an extension of the work reported in [36]. An attempt has been made to show how non-linearities could affect the heat diffusion and temperature distributions. For this purpose, the author developed a Finite Element software package and executed it on the DEC 1090 system.

An initial boundary value problem was selected and solved for non-linear material behaviour. Polynomials were used to represent the nature of non-linearity and the entire exercise was carried out for two different sets of materials. It was found that non-linearities could significantly alter the temperature distributions.

Chapter 2

FORMULATION AND ANALYSIS

2.1 THE FIELD PROBLEM

A large class of field problems are governed by similar partial differential equations for the field variable ϕ . Heat conduction, wave propagation and convective diffusion are three examples.

Consider that it is desired to evaluate the field variable ϕ in a three dimensional solution domain Ω , bounded by surface S (Fig. 2.1). The field equation to be solved could, in general, be written as,

$$\frac{\partial}{\partial x} (K_x \frac{\partial \phi}{\partial x}) + \frac{\partial}{\partial y} (K_y \frac{\partial \phi}{\partial y}) + \frac{\partial}{\partial z} (K_z \frac{\partial \phi}{\partial z}) = f(x, y, z) \quad \dots \quad (2.1)$$

where K_x , K_y , K_z and f are given functions. The physical interpretation of the parameters in the above equation depends on the particular physical problem. Table (2.1) lists some typical problems and their parameters.

The boundary conditions of (2.1) could be written as,

$$\phi = \phi(x, y, z) \text{ on } S_1 \quad (2.2)$$

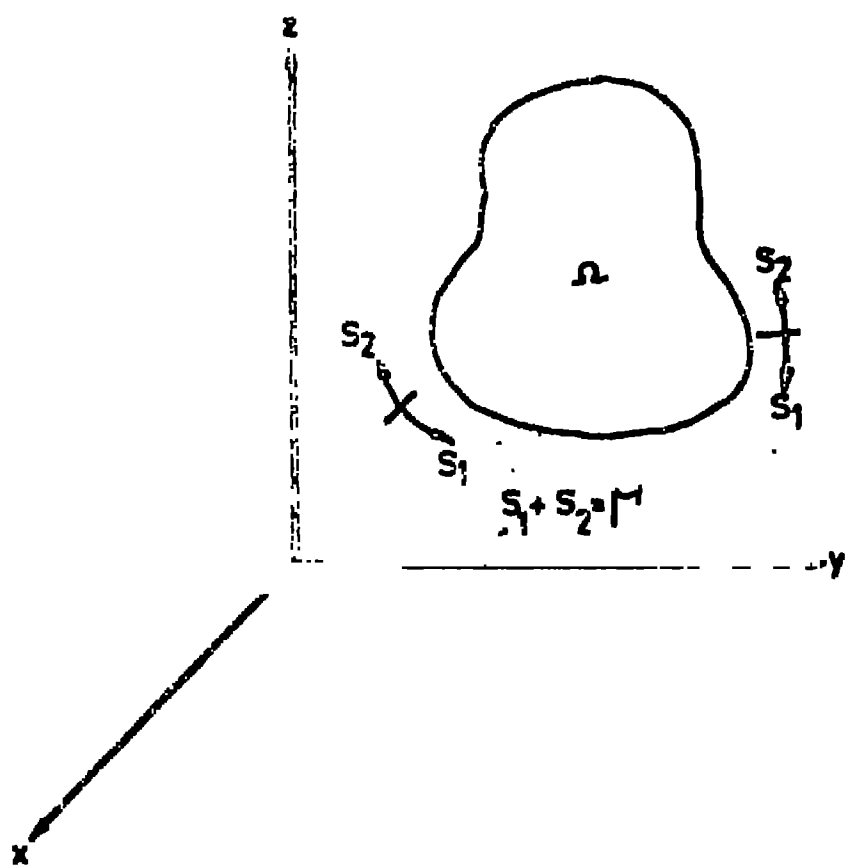


Fig. 2.1 - 3-D SOLUTION DOMAIN

No.	Problem	Field parameter ϕ	K_x, K_y, K_z	f	g	h
1.	Diffusion-flow in porous media	Hydraulic head	Hydraulic conductivity	Internal source flow	Boundary flow	-
2.	Electric conduction	Voltage	Electric conductivity	Internal current source	Externally applied boundary current	-
3.	Electro-static field	Electric force field intensity	Permitivity	Internal current source	-	-
4.	Heat conduction	Temperature	Thermal conductivity	Internal heat generation	Boundary heat generation	Conductive heat transfer coefficient
5.	Torsion	Stress function	Reciprocal of shear modulus	Angle of twist per unit length	-	-
6.	Seepage	Pressure	Permeability	Internal flow source	-	-
7.	Magnetostatics	Magnomotive force	Magnetic permeability	Internal magnetic field source	Externally applied magnetic field intensity	-

TABLE 2.1 : IDENTIFICATION OF PHYSICAL PARAMETERS

and

$$K_x \frac{\partial \phi}{\partial x} n_x + K_y \frac{\partial \phi}{\partial y} n_y + K_z \frac{\partial \phi}{\partial z} n_z + g(x, y, z) + h(x, v, z) = 0 \text{ on } S_2 \quad (2.3)$$

where g and h are known apriori and n_x , n_y , n_z are the direction cosines of the outward normal to the surface.

2.2 FORMULATION

2.2.1 Composition

Consider a two phase material whose phases are of cylindrical shape, with all generators oriented in the same direction. For convenience, let us concern ourselves with materials of cylindrical shape with generators parallel to the phase region generators. It is also assumed that phase cylindrical regions are uninterrupted along their lengths.

In the general fiber reinforced material, there is no specific geometrical distinction between the two phases. If we consider one of the phases as consisting of cylinders embedded in another phase, we will call the embedded cylinders the FIBRES and the phase in which they are embedded, the MATRIX.

2.2.2 Geometry

If we assume the fibers to be of a specific shape (in this case circular, say), the geometry is one of regular arrays of identical fibers in a matrix. The most general kinds of arrays are perhaps the square, rectangular and hexagonal arrays.

For the present study, we consider a hexagonal array of circular, cylindrical fibers (constituent-1) in a matrix (constituent-2), as shown in Fig. 2.2.

Using cylindrical polar coordinates, the domain could be described as occupying a space $0 \leq x \leq L$, $0 \leq r \leq \infty$, $0 \leq \theta \leq 2\pi$ (Fig. 2.3).

2.2.3 Formulation

We consider the temperature or heat flux boundary conditions at $x = 0$ and at $x = L$ to be such that the temperature distribution is similar in each hexagonal cell. As a consequence, the external boundary of the unit cell becomes a line of symmetry, and the component of the heat flux normal to the boundary vanishes. It is further assumed that there is no thermal resistance across the fiber-matrix interface.

To describe the heat conduction in a typical unit cell, the hexagonal boundary is approximated by a

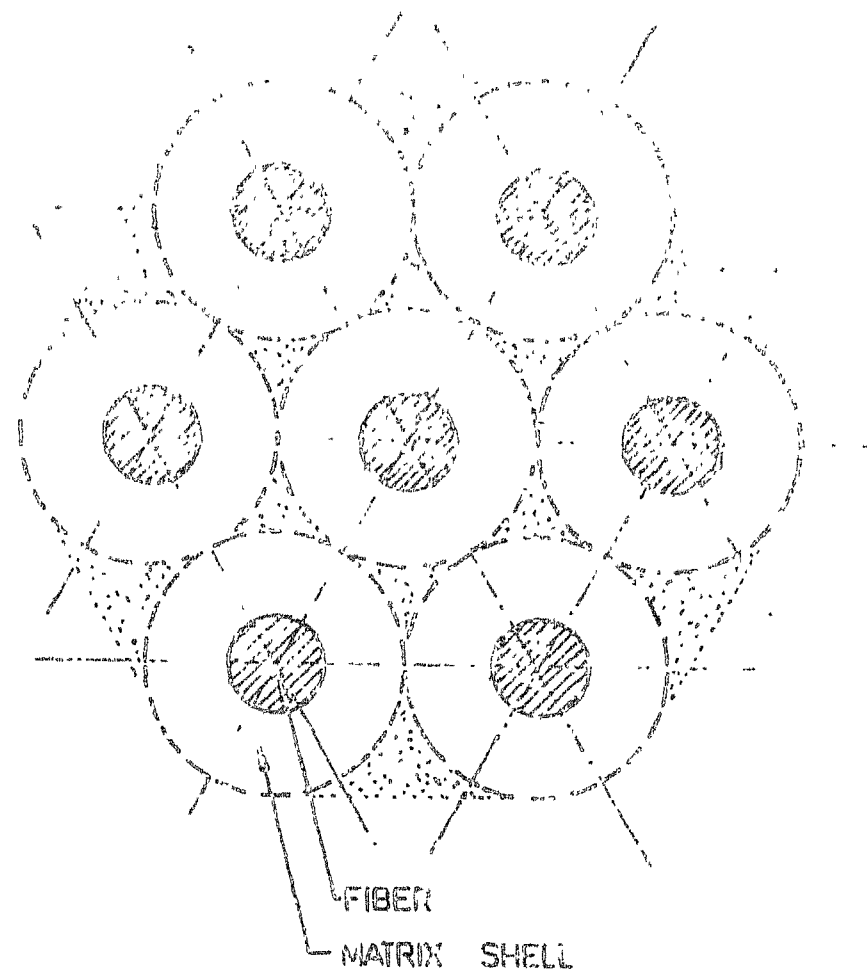


Fig. 2.2 - HEXAGONAL ARRAY -
COMPOSITE CYLINDER CONSTRUCTION

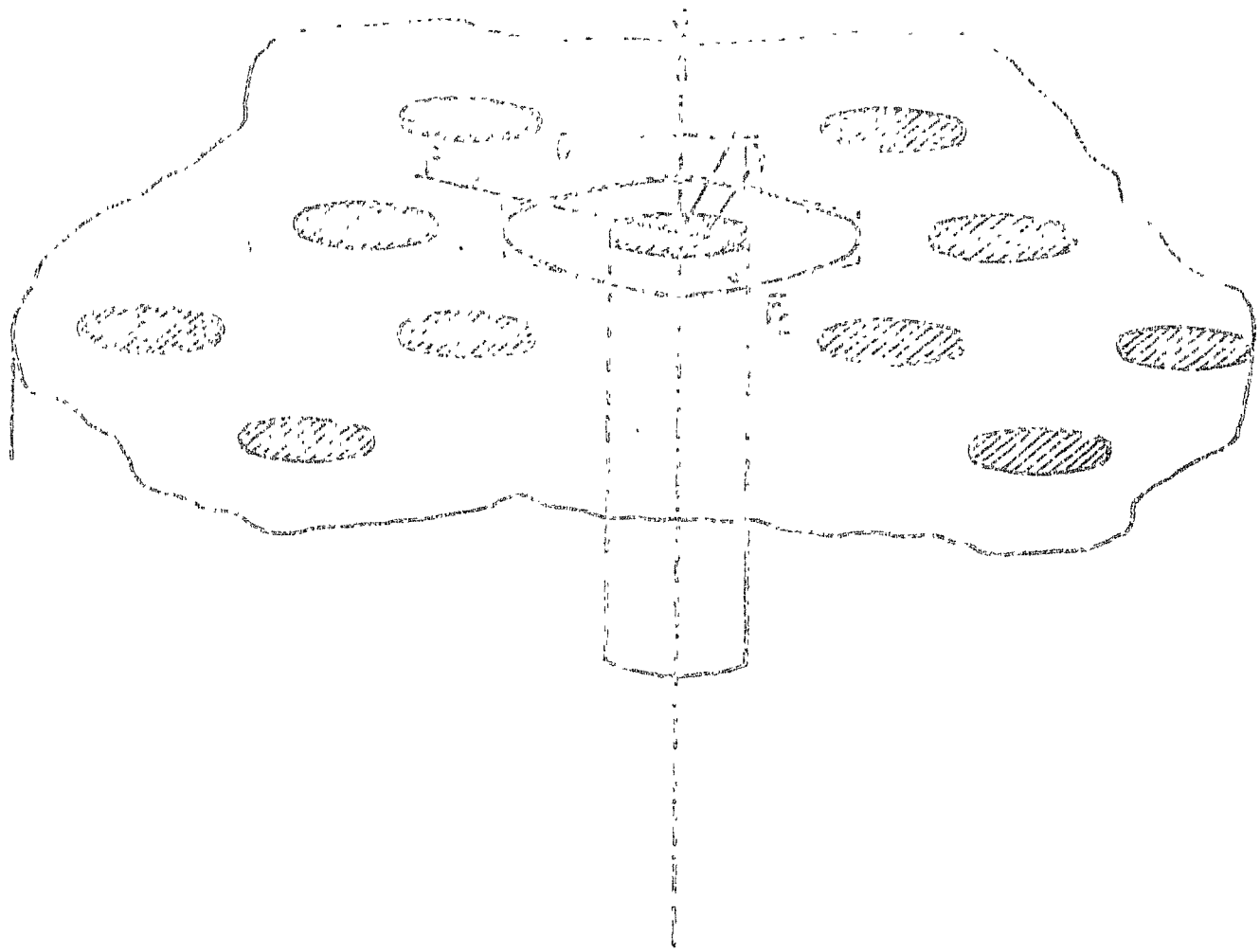


Fig. 2.3 - GEOMETRY AND COORDINATE SYSTEM

circle. As a result, the temperature distribution within the cell is axisymmetric with zero heat flux normal to the outer circular boundary of the matrix.

The initial boundary value problem that describes transient heat conduction in the cell is then given by the following equations:

(a) Conservation of energy

$$-\frac{1}{r} \frac{\partial}{\partial r} (r q_r^{(\alpha)}) - \frac{\partial}{\partial x} (q_x^{(\alpha)}) = \mu^{(\alpha)} \frac{\partial T^{(\alpha)}}{\partial t} \quad \dots \quad (2.4)$$

(b) Constitutive equations

$$q_x^{(\alpha)} = -K_x^{(\alpha)} \frac{\partial T^{(\alpha)}}{\partial x} \quad (2.5a)$$

$$q_r^{(\alpha)} = -K_r^{(\alpha)} \frac{\partial T^{(\alpha)}}{\partial r} \quad (2.5b)$$

(c) Interface conditions

$$T^{(1)}(x, r_1, t) = T^{(2)}(x, r_1, t) \quad (2.6a)$$

$$q_r^{(1)}(x, r_1, t) = q_r^{(2)}(x, r_1, t) \quad (2.6b)$$

(d) Symmetry condition

$$q_r^{(2)}(x, r_2, t) = 0 \quad (2.7)$$

(e) Initial and boundary data.

The quantities $q_r^{(\alpha)}$, $q_x^{(\alpha)}$, $\mu^{(\alpha)}$, $T^{(\alpha)}$, $K_x^{(\alpha)}$ and $K_r^{(\alpha)}$ in the above equations are, respectively, the heat flux components, heat capacity, temperature and

thermal conductivity components of the α ($\equiv 1$ or 2) constituent.

The problem has been solved to determine the evolution of the temperature field in the half space $x \geq 0$ subject to a step function at the boundary,

$$T(0, r, t) = T_0, \quad 0 \leq t \leq t_0 \quad (2.3)$$

$$0, \quad t > t_0$$

2.3 FINITE ELEMENT FORMULATION

The governing equations for the axisymmetric heat conduction problem could be written as

$$\frac{1}{r} \frac{\partial}{\partial r} (K_r r \frac{\partial T}{\partial r}) + \frac{\partial}{\partial x} (K_x \frac{\partial T}{\partial x}) = \mu \frac{\partial T}{\partial t} \quad (2.9)$$

along with its boundary conditions (Fig. 2.4).

As we consider the temperature evolution in the half space $x \geq 0$, the boundary conditions at the two ends become

$$\text{At } x = 0 \quad T = T_0, \quad 0 \leq t \leq t_0 \quad (2.10)$$

$$= 0, \quad t > t_0$$

$$\text{At } x = L \quad \frac{\partial T}{\partial x} = 0$$

By symmetry of the composite cylinder assembly, the heat flux normal to the cylindrical surface of the unit cell vanishes. Thus,

$$\text{at } r = r_2 \quad \frac{\partial T}{\partial r} = 0 \quad (2.11)$$

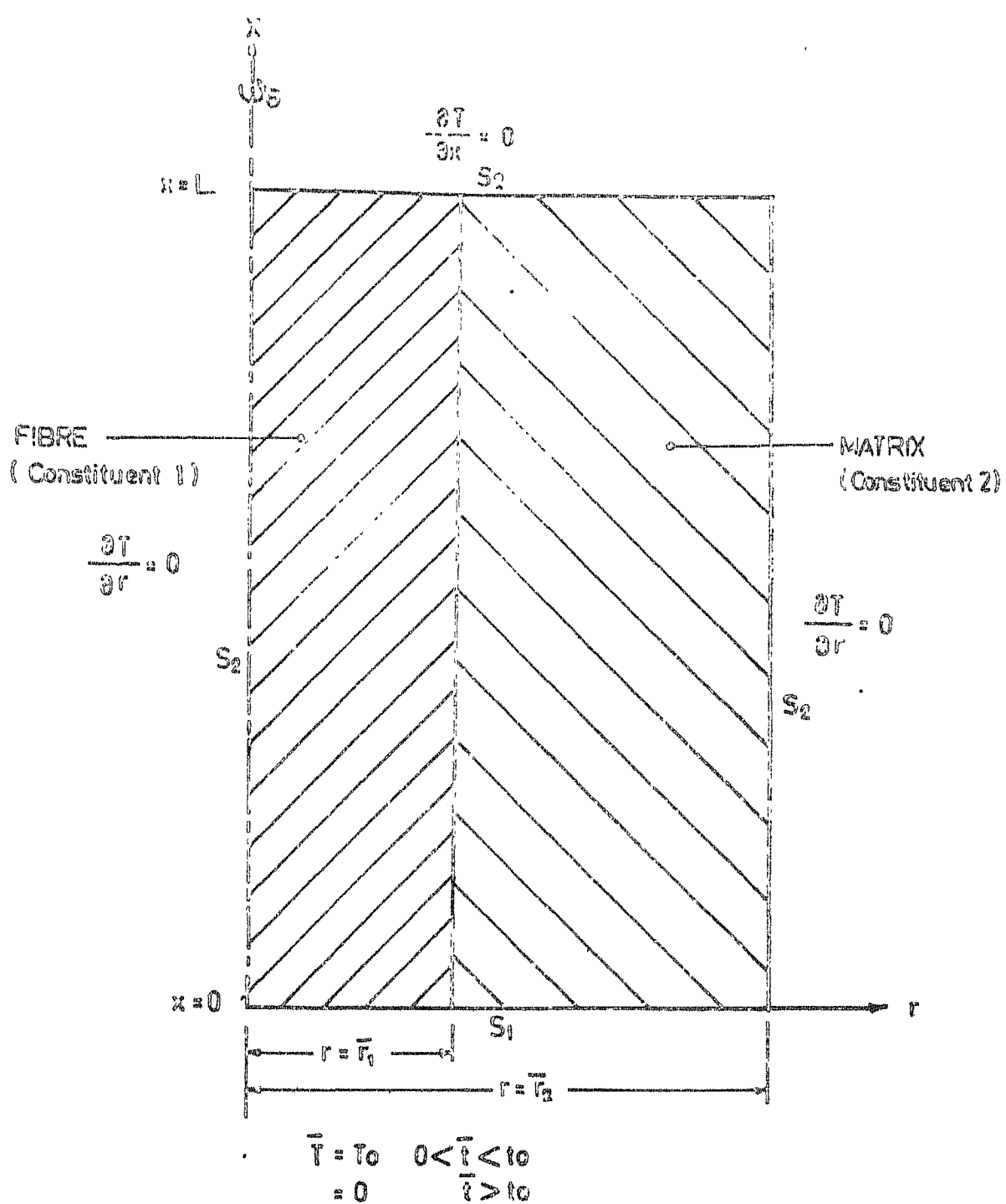


Fig. 2.4 - SYMMETRICAL HALF CROSS SECTION AND BOUNDARY CONDITIONS

Due to the symmetry of the geometry and boundary conditions, it would suffice, if analysis were carried out for one half of the cylindrical cross-section. Thus, due to symmetry,

$$\text{at } r = 0, \frac{\partial T}{\partial r} = 0 \text{ and } T \text{ is finite} \quad (2.12)$$

We shall resort to the Galerkin's approach to derive the FEM equations.

2.3.1 Finite Element Discretization

Without deciding about the type of element to use, we can write

$$\begin{aligned} T^{(e)}(x, r, t) &= \{N_i(x, r)\}^T \{T(t)\}^{(e)} \\ &= \{N\}^T \{T\}^{(e)} \end{aligned} \quad (2.13)$$

where, the interpolating functions N_i need to preserve C^0 continuity only i.e., continuity of the field variable at the element interfaces.

The Galerkin's criterion could then be applied to obtain

$$\int_{D^{(e)}} N_i \left[\frac{1}{r} \frac{\partial}{\partial r} (K_r r \frac{\partial T^{(e)}}{\partial r}) + \frac{\partial}{\partial x} (K_x \frac{\partial T^{(e)}}{\partial x}) - \mu \frac{\partial T}{\partial t} \right] dD^{(e)} = 0 \quad (2.14)$$

where $i = 1, 2, \dots, n$ and $D^{(e)}$ is the domain of element 'e'.

For axisymmetry,

$$dD^{(e)} = 2 \pi r dA^{(e)} \quad (2.15)$$

Using this in (2.14), we get,

$$\iint_D^{(e)} N_i \left[\frac{1}{r} \frac{\partial}{\partial r} (K_r r \frac{\partial T^{(e)}}{\partial r}) + \frac{\partial}{\partial x} (K_x r \frac{\partial T^{(e)}}{\partial x}) - \mu \frac{\partial T^{(e)}}{\partial t} \right] 2 \pi r dA^{(e)} = 0 \quad (2.16)$$

Integrating, by parts, the first term w.r.t. 'r' and the second term w.r.t. 'x', combining and rearranging the terms, one obtains

$$\begin{aligned} \iint_D^{(e)} & \left[N_{i,r} (K_r r \frac{\partial T^{(e)}}{\partial r}) + N_{i,x} (K_x r \frac{\partial T^{(e)}}{\partial x}) \right] dA^{(e)} \\ & + \iint_D^{(e)} \mu r N_i \frac{\partial T^{(e)}}{\partial t} dA^{(e)} \\ & = \int_{x_{\text{bottom}}}^{x_{\text{top}}} N_i (K_r r \frac{\partial T^{(e)}}{\partial r}) \Big|_{r_{\text{left}}}^{r_{\text{right}}} dx + \\ & + \int_{r_{\text{left}}}^{r_{\text{right}}} N_i (K_x r \frac{\partial T^{(e)}}{\partial x}) \Big|_{x_{\text{bottom}}}^{x_{\text{top}}} dr \\ & \dots \dots \quad (2.17) \end{aligned}$$

or,

$$\begin{aligned} \iint_D^{(e)} & \left[N_{i,r} K_r r \frac{\partial T^{(e)}}{\partial r} + N_{i,x} K_x r \frac{\partial T^{(e)}}{\partial x} \right] dA^{(e)} + \\ & + \iint_D^{(e)} \mu r N_i \frac{\partial T^{(e)}}{\partial t} dA^{(e)} \\ & = \oint_S^{(e)} N_i (K_r r \frac{\partial T^{(e)}}{\partial r} n_r + K_x r \frac{\partial T^{(e)}}{\partial x} n_x) ds \\ & \dots \dots \quad (2.18) \end{aligned}$$

Introducing the boundary condition for flux on the element boundaries $s_2^{(e)}$, we have

$$K_r r \frac{\partial T^{(e)}}{\partial r} n_r + K_x r \frac{\partial T^{(e)}}{\partial x} n_x + r q(t) = 0 \text{ for } t > 0 \\ \dots \quad (2.19)$$

Substituting in (2.18), we get

$$\iint_{D^{(e)}} \left[N_{i,r} K_r r \frac{\partial T^{(e)}}{\partial r} + N_{i,x} K_x r \frac{\partial T^{(e)}}{\partial x} \right] dA^{(e)} + \\ + \iint_{D^{(e)}} \mu r N_i \frac{\partial T^{(e)}}{\partial t} dA^{(e)} + \oint_{S_2^{(e)}} N_i r q dS_2 = 0 \\ \dots \quad (2.20)$$

Using $T^{(e)} = \{N\}^T \quad \{\dot{T}\}^{(e)}$ from (2.13) in (2.20),

$$\iint_{D^{(e)}} \left[K_r r N_{i,r} \{N_r\}^T + K_x r N_{i,x} \{N_x\}^T \right] dA^{(e)} \{T\}^{(e)} + \\ + \iint_{D^{(e)}} [\mu r N_i \{N\}^T] dA^{(e)} \{\dot{T}\}^{(e)} \\ + \oint_{S_2^{(e)}} N_i r q dS_2^{(e)} = 0 \quad (2.21)$$

where $\dot{T} = \frac{\partial T}{\partial t}$, the time derivative of the temperature.

Casting (2.21) into the matrix form, we obtain,

$$\iint_{D^{(e)}} (K_r r \{N_r\} \{N_r\}^T + K_x r \{N_x\} \{N_x\}^T) dA^{(e)} \{T\}^{(e)} + \\ + \iint_{D^{(e)}} (\mu r \{N\} \{N\}^T) dA^{(e)} \{\dot{T}\}^{(e)} \\ + \oint_{S_2^{(e)}} \{N\} r q dS_2^{(e)} = 0 \quad (2.22)$$

or

$$[K]^{(e)} \{T\}^{(e)} + [C]^{(e)} \{\dot{T}\}^{(e)} + \{F\}^{(e)} = 0 \quad (2.23)$$

This is the basic element matrix equation.

For each element,

the thermal stiffness matrix,

$$[K]^{(e)} = \iint_{D^{(e)}} (K_r r \{N, r\} \{N, r\}^T + K_x r \{N, x\} \{N, x\}^T) dA^{(e)} \quad (2.24)$$

the thermal capacitance matrix

$$[C]^{(e)} = \iint_{D^{(e)}} \mu r \{N\} \{N\}^T dA^{(e)} \quad (2.25)$$

and the heat flux matrix

$$[F]^{(e)} = \oint_{S_2^{(e)}} r q^{(e)} ds_2^{(e)} \quad (2.26)$$

Our problem is an axisymmetric case, which requires continuity of the field variable alone. Let us choose triangular ring elements (Figs. 2.5, 2.6) with linear variation of field variable T along the element boundaries as it satisfies both C^0 compatibility and completeness requirements. For the three node element we have,

$$T^{(e)}(x, r, t) = \begin{Bmatrix} \eta_1 \\ \eta_2 \\ \eta_3 \end{Bmatrix}^T \begin{Bmatrix} T_1(t) \\ T_2(t) \\ T_3(t) \end{Bmatrix} \quad (2.27)$$

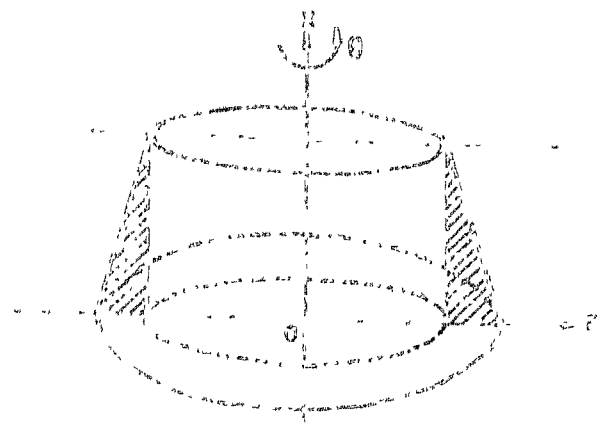


Fig. 2.5 - TRIANGULAR RING ELEMENT

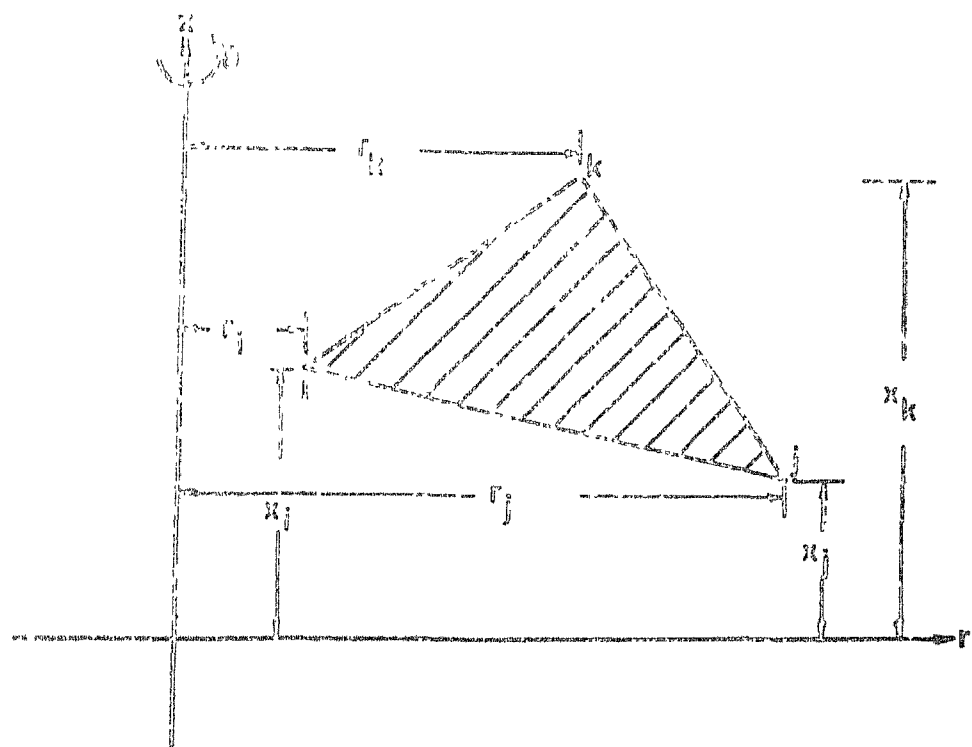


Fig. 2.6 - SECTION AND CO-ORDINATES OF RING ELEMENT (TRIANGULAR)

For linear variation of T along the element boundaries,

$$\eta_1 = N_1 = \frac{(r_i x_j - r_j x_i) + (r_j x_k - r_k x_j) + (r_k x_i - r_i x_k)}{(r_i x_j - r_j x_i) + (r_j x_k - r_k x_j) + (r_k x_i - r_i x_k)}$$

The denominator of η_1 is equal to $2A$ where A is the area of the triangle. Likewise, it is also the denominator of η_2 and η_3 .

Hence,

$$\eta_2 = N_2 = \frac{(r_i x - r x_i) + (r x_k - r_k x) + (r_k x_i - r_i x_k)}{2A}$$

and

$$\eta_3 = N_3 = \frac{(r_i x_j - r_j x_i) + (r_j x - r x_j) + (r x_i - r_i x)}{2A} \dots \quad (2.28)$$

Also,

$$\eta_1 + \eta_2 + \eta_3 = N_1 + N_2 + N_3 = 1$$

We have as a consequence of the above definitions,

$$\begin{aligned} N_{1,r} &= \frac{\partial N_1}{\partial r} = \frac{(x_j - x_k)}{2A} = \frac{B_1}{2A} \\ N_{2,r} &= \frac{\partial N_2}{\partial r} = \frac{(x_k - x_i)}{2A} = \frac{B_2}{2A} \\ N_{3,r} &= \frac{\partial N_3}{\partial r} = \frac{(x_i - x_j)}{2A} = \frac{B_3}{2A} \end{aligned} \quad (2.29)$$

where B_1 , B_2 and B_3 are constants.

Likewise,

$$\begin{aligned} N_{1,x} &= \frac{\partial N_1}{\partial x} = \frac{(r_k - r_j)}{2A} = \frac{C_1}{2A} \\ N_{2,x} &= \frac{(r_i - r_k)}{2A} = \frac{C_2}{2A} \end{aligned}$$

$$N_{3,x} = \frac{(r_j - r_i)}{2A} = \frac{C_3}{2A} \quad (2.30)$$

where C_1 , C_2 and C_3 are constants.

We now proceed to evaluate the elemental matrices.

(i) Thermal conductivity (stiffness) matrix:

We have

$$[K]^{(e)} = \iint_{D^{(e)}} (K_r r \{N, r\} \{N, r\}^T + K_x r \{N, x\} \{N, x\}^T) dA^{(e)} \quad (2.24)$$

Our thermal conductivity K is temperature dependent for its value. As suggested by Abel and Desai [46], assuming piecewise linearity for K i.e., a constant but different thermal conductivity for each increment, we could proceed as though the case were linear. Using this ideology and substituting for N , r and N, x from (2.29) and (2.30) we obtain,

$$[K]^{(e)} = \iint_{D^{(e)}} \left(\frac{k_r r}{4A^{(e)2}} \begin{Bmatrix} B_1 \\ B_2 \\ B_3 \end{Bmatrix} \begin{Bmatrix} B_1 \\ B_2 \\ B_3 \end{Bmatrix}^T + \frac{K_x r}{4A^{(e)2}} \begin{Bmatrix} C_1 \\ C_2 \\ C_3 \end{Bmatrix} \begin{Bmatrix} C_1 \\ C_2 \\ C_3 \end{Bmatrix}^T \right) dA^{(e)} \quad (2.31)$$

Algebraic manipulation will prove $r = r_i \eta_1 + r_j \eta_2 + r_k \eta_3$

Hence,

$$[K]^{(e)} = \iint_D^{(e)} \frac{K}{4A^{(e)2}} \begin{bmatrix} B_1^2 + C_1^2 & B_1 B_2 + C_1 C_2 & B_1 B_3 + C_1 C_3 \\ & B_2^2 + C_2^2 & B_2 B_3 + C_2 C_3 \\ \text{Symm.} & & B_3^2 + C_3^2 \end{bmatrix} (r_i \eta_1 + r_j \eta_2 + r_k \eta_3) dA^{(e)} \dots \quad (2.32)$$

For a triangular element, the integration formula is

$$\iint_A^{(e)} \eta_1^\alpha \eta_2^\beta \eta_3^\gamma dA^{(e)} = \frac{(\alpha! \beta! \gamma!)}{(\alpha + \beta + \gamma + 2)!} 2A \dots \quad (2.33)$$

Employing this, (2.32) transforms to

$$[K]^{(e)} = \frac{K^{(e)}}{4A^{(e)2}} \begin{bmatrix} B_1^2 + C_1^2 & B_1 B_2 + C_1 C_2 & B_1 B_3 + C_1 C_3 \\ & B_2^2 + C_2^2 & B_2 B_3 + C_2 C_3 \\ \text{Symm.} & & B_3^2 + C_3^2 \end{bmatrix} \iint_D^{(e)} (r_i \eta_1 + r_j \eta_2 + r_k \eta_3) dA^{(e)} \\ [K]^{(e)} = \frac{K^{(e)}}{12A^{(e)2}} \begin{bmatrix} B_1^2 + C_1^2 & B_1 B_2 + C_1 C_2 & B_1 B_3 + C_1 C_3 \\ & B_2^2 + C_2^2 & B_2 B_3 + C_2 C_3 \\ & & B_3^2 + C_3^2 \end{bmatrix} (r_i + r_j + r_k) \quad (2.34)$$

In equations (2.26) and (2.28), $k^{(e)}$ has been used as if it were a constant and equal in both axial and radial directions. This has been done for convenience of expression. During solution, it is necessary to club the value of radial conductivity with the 'B' terms and axial conductivity with the 'C' terms.

(ii) Thermal capacitance matrix:

We have

$$[C]^{(e)} = \iint_{D^{(e)}} \mu r \{N\} \{N\}^T dA^{(e)} \quad (2.25)$$

Extending the argument of piecewise linearity to the thermal capacitance and considering it constant over an element, we have

$$\begin{aligned} [C]^{(e)} &= \mu^{(e)} \iint_{D^{(e)}} \{N\} \{N\}^T (r_i \eta_1 + r_j \eta_2 + r_k \eta_3) dA^{(e)} \\ &= \mu^{(e)} \iint_{D^{(e)}} \begin{bmatrix} \eta_1^2 & \eta_1 \eta_2 & \eta_1 \eta_3 \\ \eta_2 \eta_1 & \eta_2^2 & \eta_2 \eta_3 \\ \eta_3 \eta_1 & \eta_3 \eta_2 & \eta_3^2 \end{bmatrix} (r_i \eta_1 + r_j \eta_2 + r_k \eta_3) dA^{(e)} \end{aligned}$$

Employing the integration formula, this reduces to

$$[C]^{(e)} = \frac{\mu^{(e)} A^{(e)}}{60} \begin{bmatrix} (6r_i + 2r_j + 2r_k) & (2r_i + 2r_j + r_k) & (2r_i + r_j + 2r_k) \\ & (2r_i + 6r_j + 2r_k) & (r_i + 2r_j + 2r_k) \\ \text{Symm.} & & (2r_i + 2r_j + 6r_k) \\ \dots & & \dots \end{bmatrix} \quad (2.35)$$

(iii) Element heat flux vector:

From (2.26),

$$\{F\}^{(e)} = \oint_{S_2^{(e)}} \{N\}^T r q^{(e)} ds_2^{(e)}$$

This term exists only for elements at the boundary where the heat flux is specified. Consider that on the boundary edge the heat flux is constant for any element. This assumption simplifies the analysis.

Thus,

$$\begin{aligned} \{F\}^{(e)} &= q^{(e)}(t) \oint_{S_2^{(e)}} \{N\}^T r ds_2^{(e)} \\ &= q^{(e)}(t) \oint_{S_2^{(e)}} \begin{Bmatrix} n_1 \\ n_2 \end{Bmatrix} (r_i n_1 + r_j n_2) ds_2^{(e)} \\ &= q^{(e)}(t) \oint_{S_2^{(e)}} \begin{Bmatrix} r_i n_1^2 + r_j n_1 n_2 \\ r_i n_1 n_2 + r_j n_2^2 \end{Bmatrix} ds_2^{(e)} \\ &\dots \end{aligned} \quad (2.36)$$

For a linear element, the appropriate integration formula is

$$\phi_{(e)} \eta_1^\alpha \eta_2^\beta = \frac{\alpha! \beta!}{(\alpha+\beta+1)!} s_{1-2}$$

where s_{1-2} is the length of the linear element.

Using this, (3.36) transforms to,

$$\{F\}^{(e)} = q^{(e)}(t) s_{i-j} \begin{Bmatrix} r_i/3 + r_j/6 \\ r_i/6 + r_j/3 \end{Bmatrix} \quad (2.37)$$

where s_{i-j} is the length of the boundary edge of the element.

2.3.2 General Matrix Equations

The element matrices as given above are calculated for each element and assembled together to give the system of simultaneous linear equations in the matrix form as

$$[K] \{T\} + [C] \{\dot{T}\} + \{F\} = 0 \quad (2.38)$$

Our problem being a transient case, we are confronted with time derivatives of temperatures. Zienkiewicz [37] shows that either finite difference approximations or finite elements in time (use a shape function defined in the time domain) may be used for computer solution and that the methods are equivalent.

We will adopt the former method, replacing time derivatives by finite difference approximations.

From (3.38) at time t ,

$$[K_t] \{T_t\} + [c_t] \{\dot{T}_t\} + \{F_t\} = 0 \quad (2.39)$$

At time $t-\delta t$

$$[K_{t-\delta t}] \{T_{t-\delta t}\} + [c_{t-\delta t}] \{\dot{T}_{t-\delta t}\} + \{F_{t-\delta t}\} = 0 \quad \dots \quad (2.40)$$

Then,

$$\{T_t\} = \{T_{t-\delta t}\} + \frac{\delta t}{2} \{\dot{T}_t\} + \frac{\delta t}{2} \{\dot{T}_{t-\delta t}\}$$

Or,

$$\{\dot{T}_t\} = \frac{2}{\delta t} (\{T_t\} - \{T_{t-\delta t}\}) - \{\dot{T}_{t-\delta t}\} \quad (2.41)$$

Substituting equation (2.41) in (2.39) we have,

$$\begin{aligned} [K_t] \{T_t\} + [c_t] \left(\frac{2}{\delta t} (\{T_t\} - \{T_{t-\delta t}\}) - \{\dot{T}_{t-\delta t}\} \right) \\ + \{F_t\} = 0 \end{aligned}$$

Or,

$$\begin{aligned} ([K_t] + \frac{2}{\delta t} [c_t]) \{T_t\} = [c_t] \left(\{\dot{T}_{t-\delta t}\} + \frac{2}{\delta t} \{T_{t-\delta t}\} \right) \\ - \{F_t\} \end{aligned} \quad (2.42)$$

From (2.40),

$$\{\dot{T}_{t-\delta t}\} = [c_{t-\delta t}]^{-1} (-[K_{t-\delta t}] \{T_{t-\delta t}\} - \{F_{t-\delta t}\}) \quad \dots \quad (2.43)$$

Substituting this in (2.42), we obtain,

$$\begin{aligned} ([K_t] + \frac{2}{\delta t} [c_t]) \{T_t\} = [c_t] (-[c_{t-\delta t}]^{-1} [K_{t-\delta t}] \{T_{t-\delta t}\} \\ - [c_{t-\delta t}]^{-1} \{F_{t-\delta t}\}) + [c_t] \frac{2}{\delta t} \{T_{t-\delta t}\} - \{F_t\} \end{aligned}$$

Rearranging,

$$\begin{aligned}
 & ([\kappa_t] + \frac{2}{\delta t} [c_t]) \{T_t\} = (\frac{2}{\delta t} [c_t] - \\
 & - [c_t] [c_{t-\delta t}]^{-1} [\kappa_{t-\delta t}]) \{T_{t-\delta t}\} \\
 & - [c_t] [c_{t-\delta t}]^{-1} \{F_{t-\delta t}\} - \{F_t\} \quad (2.44)
 \end{aligned}$$

For most materials the variation of thermal conductivity with temperature is much more pronounced than that of the thermal capacity. Considering, therefore, that this variation be neglected in comparison, we can write

$$[c_{t-\delta t}] = [c_t] = [c] \quad (2.45)$$

$$\begin{aligned}
 \therefore ([\kappa_t] + \frac{2}{\delta t} [c]) \{T_t\} &= (\frac{2}{\delta t} [c] - [\kappa_{t-\delta t}]) \{T_{t-\delta t}\} \\
 &- (\{F_t\} + \{F_{t-\delta t}\}) \quad (2.46)
 \end{aligned}$$

This equation is valid for transient analysis. For steady state problems, the time derivative of temperature is zero, reducing (2.38) to the form of the Fourier law of conduction,

$$[\kappa] \{T\} + \{F\} = 0 \quad (2.47)$$

Solution of this equation gives the steady state results in one step of computation.

2.4 SOLUTION PACKAGE

A computer program has been formulated to solve the matrix equations in FORTRAN. The program enables holding of boundary nodes at constant temperatures.

As we are solving for the temperature field, it would be of interest to suppress the nodes for which the temperature is already known.

We have the equation

$$[[K] + \frac{2}{\delta t} [C]] \{T_t\} = [\frac{2}{\delta t} [C] - [K_{t-\delta t}]] \{T_{t-\delta t}\} - (\{F_t\} + \{F_{t-\delta t}\}) \quad (2.46)$$

The solution procedure, essentially iterative, is as follows:

The initial temperature field being specified, the value of conductivity matrix elements is found using the specified conductivity temperature relations. Using these values of conductivity, the equation (2.46) is solved to obtain the temperature field at the end of the time interval δt . The values accruing from the new temperature field are then the basis for calculation of conductivity values to be used in the computation of the temperature field during the succeeding iteration. The process is repeated for desired number of iterations or for the desired time period.

The matrix equation (2.46) can be rewritten to enable suppression of nodal equations with constant or fixed temperatures. Denoting the conductivity matrix by $[A]$ and the heat capacity matrix by $[B]$ we can write,

$$[A+B] \{T\} = [B-A] \{T_0\} \quad (2.48)$$

where, solution for the vector T is sought and vector ' T_0 ' is the temperature field, just computed or at the beginning of the iteration. If ' \bar{T} ' represents the fixed temperatures, (2.48) can be rewritten as,

$$\begin{aligned} & \begin{bmatrix} A_{11} + B_{11} & A_{12} + B_{12} \\ A_{21} + B_{21} & A_{22} + B_{22} \end{bmatrix} \begin{Bmatrix} T \\ \bar{T} \end{Bmatrix} \\ &= - \begin{bmatrix} A_{11} + B_{11} & A_{12} + B_{12} \\ A_{21} + B_{21} & A_{22} + B_{22} \end{bmatrix} \begin{Bmatrix} T_0 \\ \bar{T} \end{Bmatrix} \\ &+ \begin{bmatrix} 2B_{11} & 2B_{12} \\ 2B_{21} & 2B_{22} \end{bmatrix} \begin{Bmatrix} T_0 \\ \bar{T} \end{Bmatrix} \end{aligned}$$

which leads to,

$$\begin{aligned} [A_{11} + B_{11}] \{T_1\} &= - [A_{11} + B_{11}] \{T_0\} \\ &- 2 [A_{12} + B_{12}] \{\bar{T}\} + 2 [B_{11}] \{T_0\} \\ &+ 2 [B_{12}] \{\bar{T}\} \\ &= - 2 [A_{12}] \{\bar{T}\} - [A_{11} + B_{11}] \{T_0\} + 2 [B_{11}] \{T_0\} \\ \therefore [A_{11} + B_{11}] \{T_1\} &= - 2 [A_{12}] \{\bar{T}\} + [B_{11} - A_{11}] \{T_0\} \\ &\dots \end{aligned} \quad (2.49)$$

In the solution of the above equation it would be of considerably economy if use were made of the

symmetry of matrices [A] and [B]. Also, these are banded matrices, enabling one to store elements within one half the band width alone entailing thereby savings in space and computational times.

Use was made of the NAG (Numerical Algorithms Group) FORTRAN library [36] routine F04ACF for the solution of the system of equations (2.49). The triangular ring element mesh is shown in Fig. 2.7.

NO. OF ELEMENTS = 120

NO. OF NODES = 80

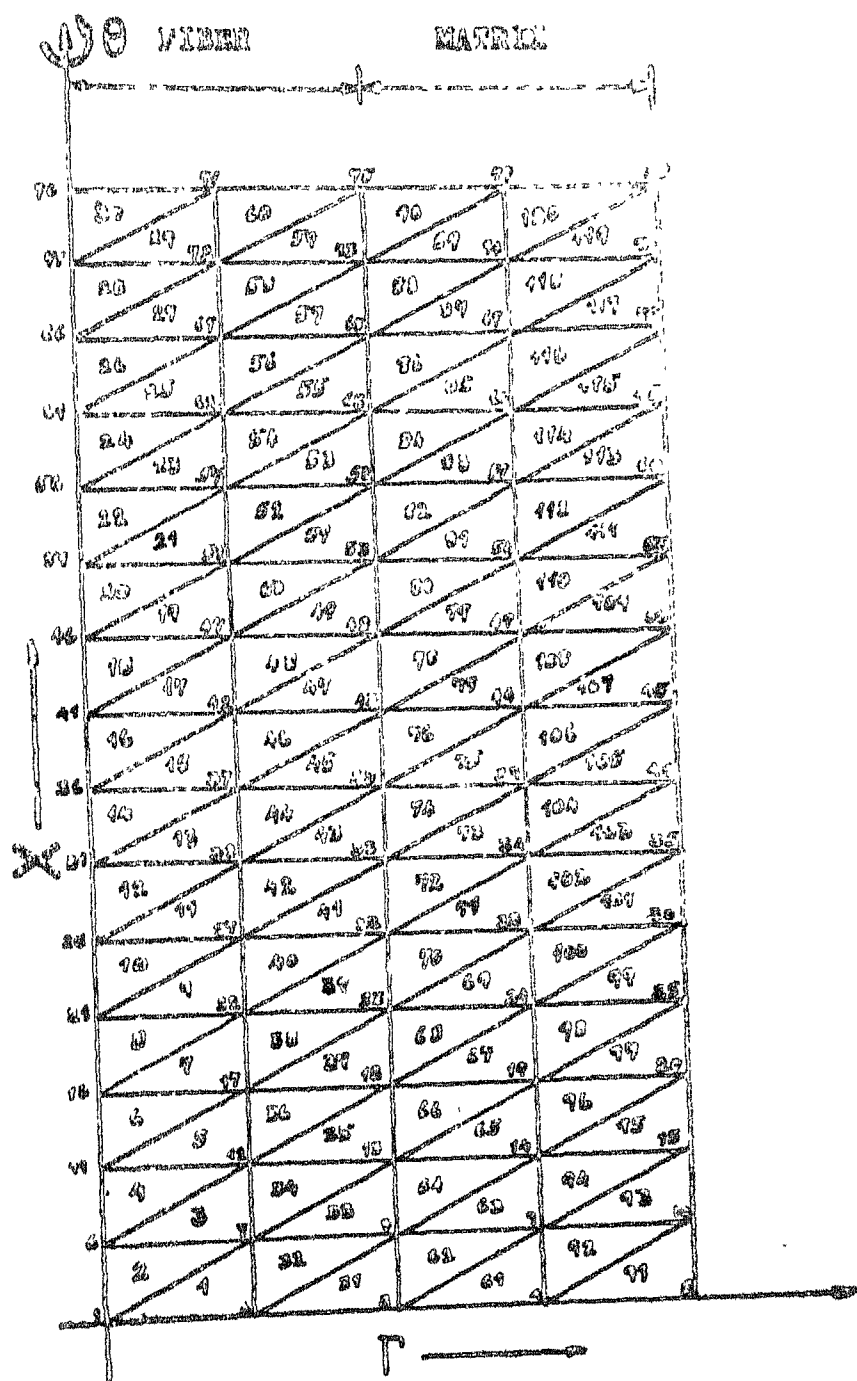


FIG. 2.7 FINITE ELEMENT MESH FOR ANALYSIS

CHAPTER 3

3.1 RESULTS AND DISCUSSIONS

The diffusion model and its finite element formulation that have been developed in the previous chapter are used to find solutions for global and micro-temperature fields in the half space $X \geq 0$, subject to a temperature-pulse boundary condition. System sensitivities to non-linearities arising from temperature dependent thermal properties have been accounted for. Two sets of materials, Graphite/Epoxy and carbon/carbon composites have been considered as specific examples. A FEM computer package is developed for this purpose and executed on the DEC 1090 system. This is attached as Appendix 1. The results have been presented in the graphical form and are discussed below. The temperature dependence of thermal properties have been shown in Appendices 2 and 3.

The average values of the nodal temperatures at each cross-section of the fibre and the matrix have been plotted against the axial length of the Graphite/Epoxy composite, in Fig. 3.1. This has been done for a

particular instant of time just before the withdrawal of the constant temperature source at the boundary. $T^{(1)}$ represents the fiber temperature and $T^{(2)}$ the matrix temperature. It is seen that the fiber is at a higher temperature than the matrix through a major length of the composite. It tends to the matrix or composite temperature at distances away from the source. It can also be observed that the non-linearity of temperature properties provide lower temperature values in comparison to the linear case. This shows that the decrease in thermal conductivity with increase in temperature for Graphite plays a dominant role in the resulting temperature distribution.

The average temperatures as explained above have also been plotted (Fig. 3.2) for the situation just after the withdrawal of the constant temperature source in order to study the decay of the temperature fields in the two materials of the composite. Since the thermal conductivity of the matrix material is less than that of the fiber material, the temperature drop in the matrix material is much slower and consequently it is at higher temperature near the boundary. This also accounts for greater temperatures of the fiber at intermediate regions. It can be noticed that non-linearities provide for faster growth and decay of the temperature fields.

The behaviour of average temperatures $T^{(1)}$ and $T^{(2)}$ at an intermediate cross-section with the passage of time is shown in Fig. 3.3. As evident, temperature builds up and decays faster in the fiber than in the matrix accounting for the higher thermal conductivity of the fiber material. The figure also shows the difference between the linear and non-linear behaviour of the composite.

The ability of the analysis to predict the temperature microstructure is illustrated in Fig. 3.4. The figure shows the temperature fields across an intermediate cross-section a short while before and after the withdrawal of the constant temperature source.

A short while before removal of the source, the temperature across the fiber is at a higher value than that across the matrix and is practically uniform. In the matrix core, it gradually reduces from a value of the fiber temperature at the interface to a minimum at the unit cell boundary. This is due to the lower thermal conductivity of the matrix material.

A little while after removal of the source, however, the trend reverses. The fiber, having greater thermal conductivity, loses its heat faster and is consequently at a lower temperature than the matrix.

The material properties used in deriving the results discussed above represent a Graphite/Fpox fiber reinforced composite. In this case, the thermal properties depend rather weakly on temperature. The results however, imply that temperature dependence of thermal properties can significantly influence the results. In an effort to demonstrate this point, a similar initial value problem was posed and solved for a carbon/carbon composite. The material properties used in the evaluation are provided in appendix III. The following discussions reflect the observations made.

Figure 3.5 represents the temperature distribution along the axial length of the composite before withdrawal of the source. The results indicate that non-linearities have significantly altered the distributions. It is worthwhile to note that temperatures calculated by taking into consideration the non-linear material behaviour, which is representative of actual working conditions to a greater extent, are much lower than those obtained by the assumption of linear behaviour. A possible consequence of this knowledge would perhaps lead us to employ lesser insulating thicknesses than we possibly would have, entailing cost savings.

On withdrawal of the constant temperature source, the temperature distributions are greatly altered as can be seen from the figure 3.6. The figure also provides ample evidence of the effect of non-linearities on the temperature distribution. It can be observed that "non-linear" temperatures are much lower than the "linear" temperatures for most of the length of the composite.

Figure 3.7 shows the temperature time history at an intermediate cross-section of the composite. As long as the source exists, the temperatures build up. On removal of the source however, there is a decay in the temperature fields. The figure also illustrates significant deviations caused due to non-linearities in the thermal behaviour of the composite.

The temperature distribution across an intermediate section, just before, and after withdrawal of the constant temperature source are shown in figure 3.8. As expected, it is observed that the temperature builds up and decays faster across the cross-section of the fiber due to the higher thermal conductivity of the fiber material as compared to that of the matrix material.

3.2 CONCLUSIONS

The heat conduction in uni-directional fiber reinforced composites subjected to a temperature pulse has been discussed in the present work. The effect of non-linearities on the temperature distributions have been amply demonstrated. The following conclusions may be drawn:

- (i) Non-linearities arising from temperature-dependent thermal properties significantly influence the temperature distributions.
- (ii) The non-linearities in case of both Graphite/Epoxy and Carbon/Carbon, lead to temperature fields having magnitudes lower than those in the linear case..
- (iii) The non-linear analysis of the problem leads to an important result that less composite material is actually needed for insulation purposes than what is predicted by the linear solutions.
- (iv) Since the non-linear behaviour of the composite structures is a true representation of the materials used in practice, it is recommended that non-linearities must be accounted for in the heat diffusion analysis.

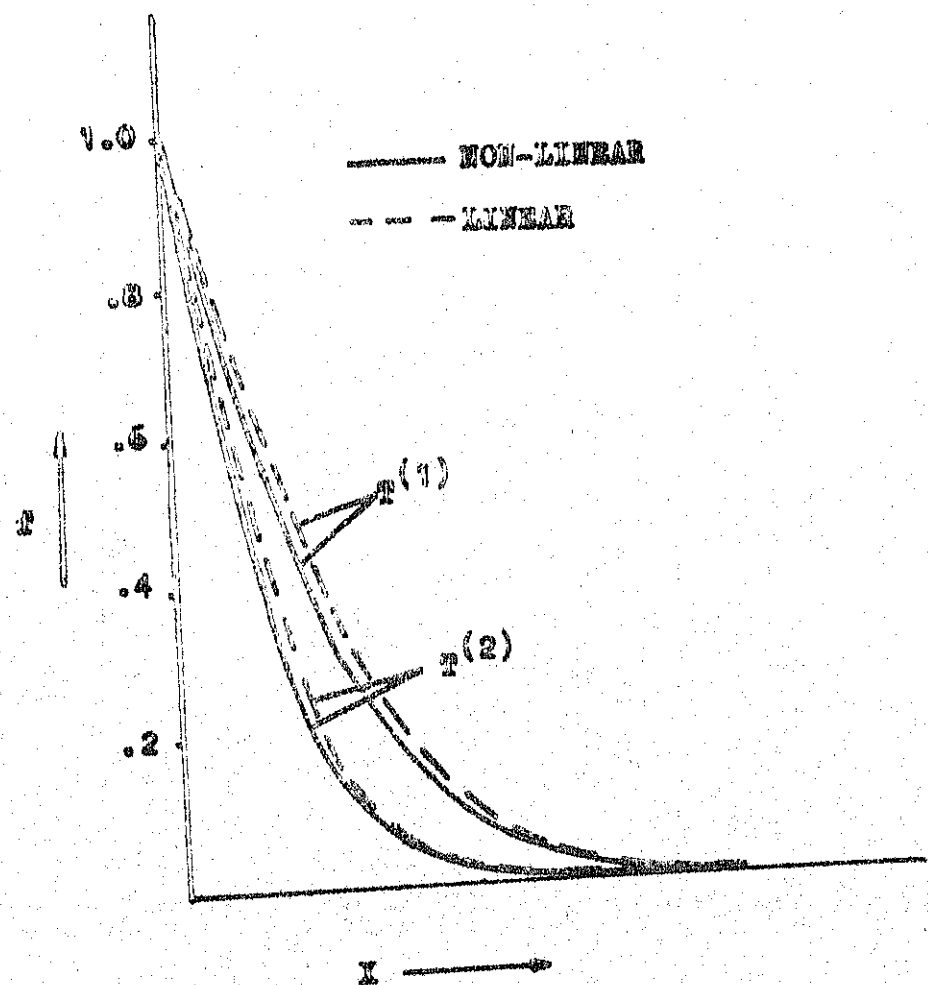


FIG. 3.1 AVERAGE AXIAL TEMPERATURE DISTRIBUTION
BEFORE WITHDRAWAL OF TEMPERATURE SOURCE
(GRAPHITE/EPOXY).

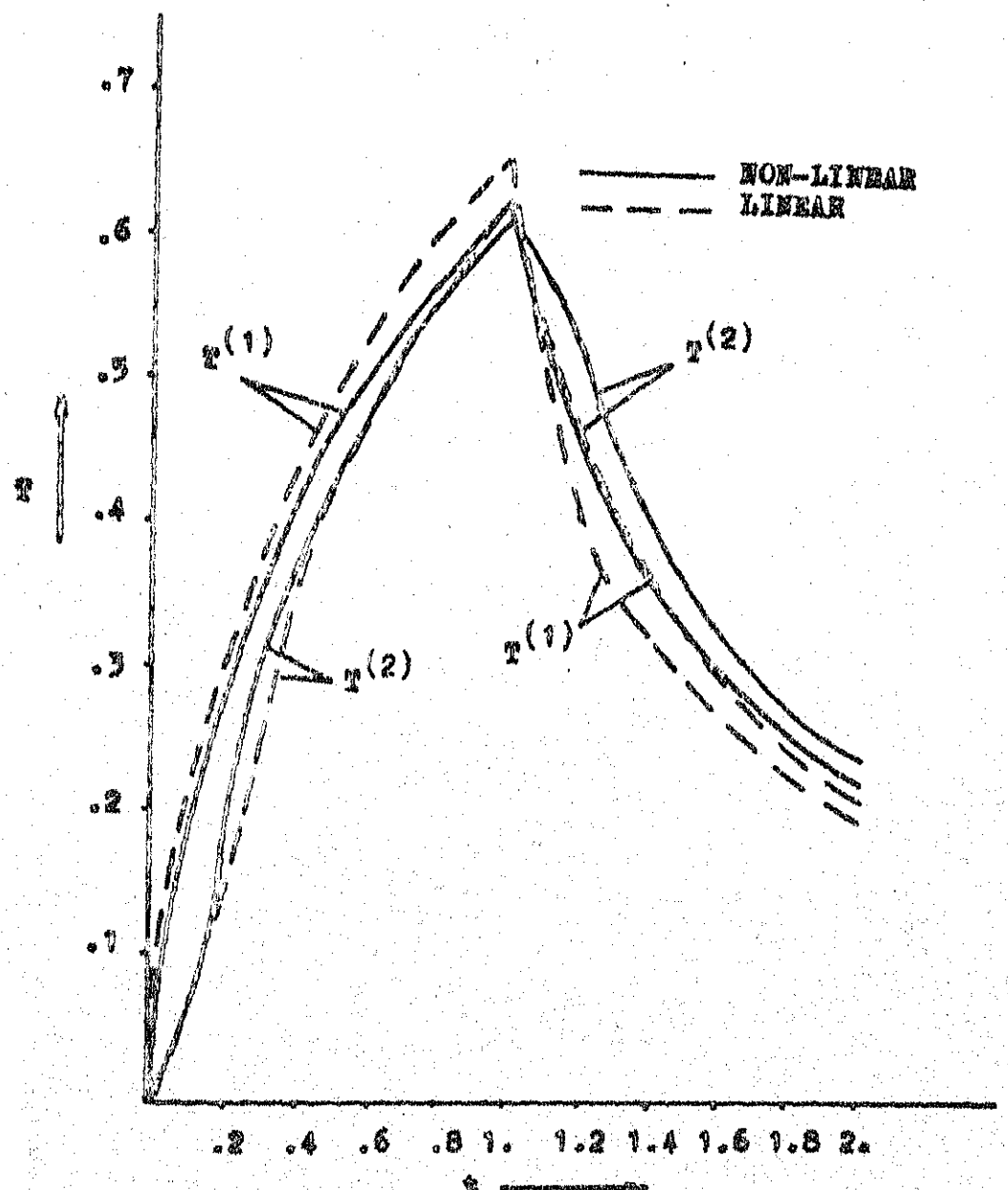


FIG. 3.9 TEMPERATURE-TIME HISTORY AT AN INTERMEDIATE REGION (GRAPHITE/EPOXY).

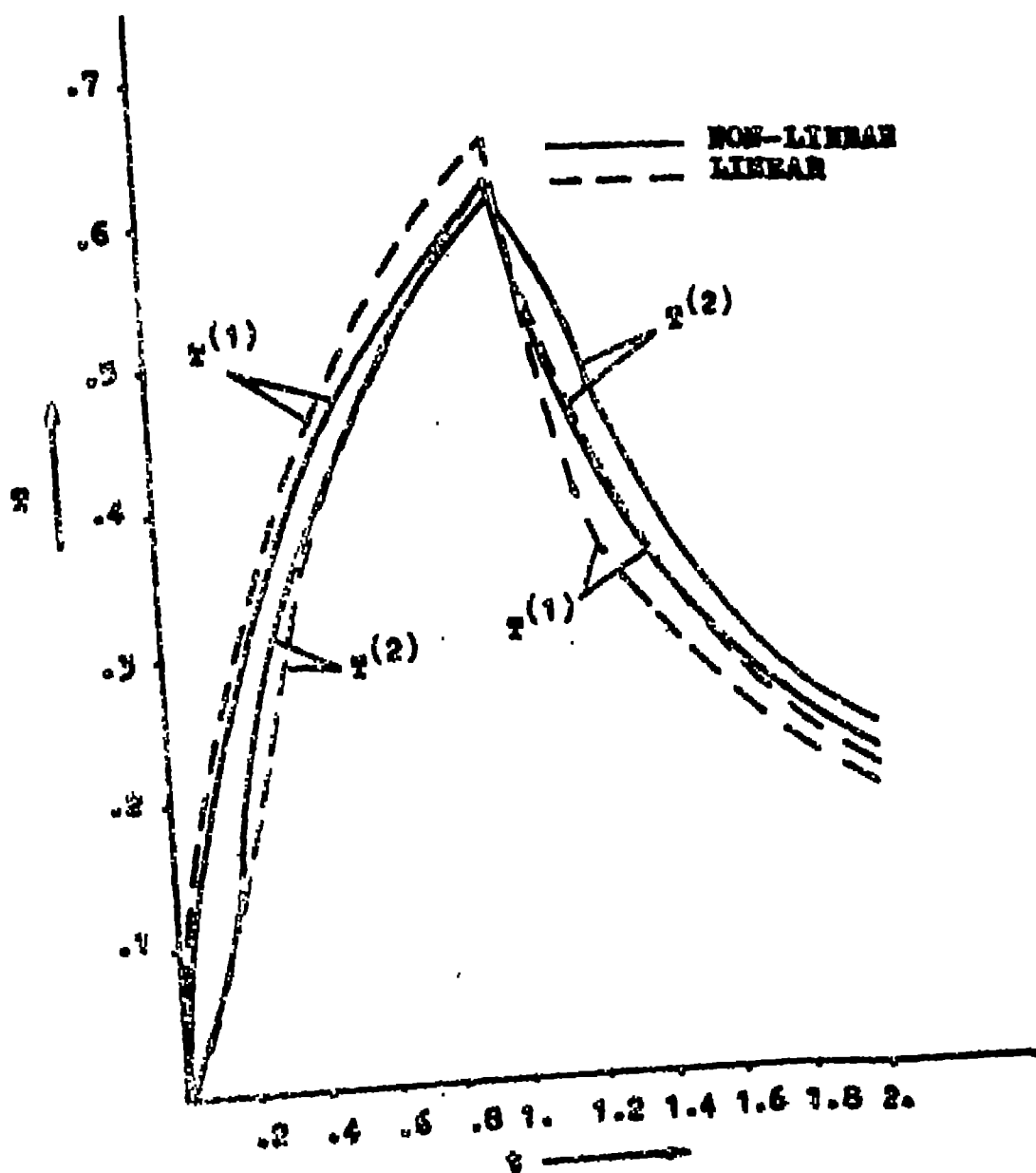


Fig. 3.3 TEMPERATURE-TIME HISTORY AT AN INTERMEDIATE REGION (GRAPHITE/EPOXY).

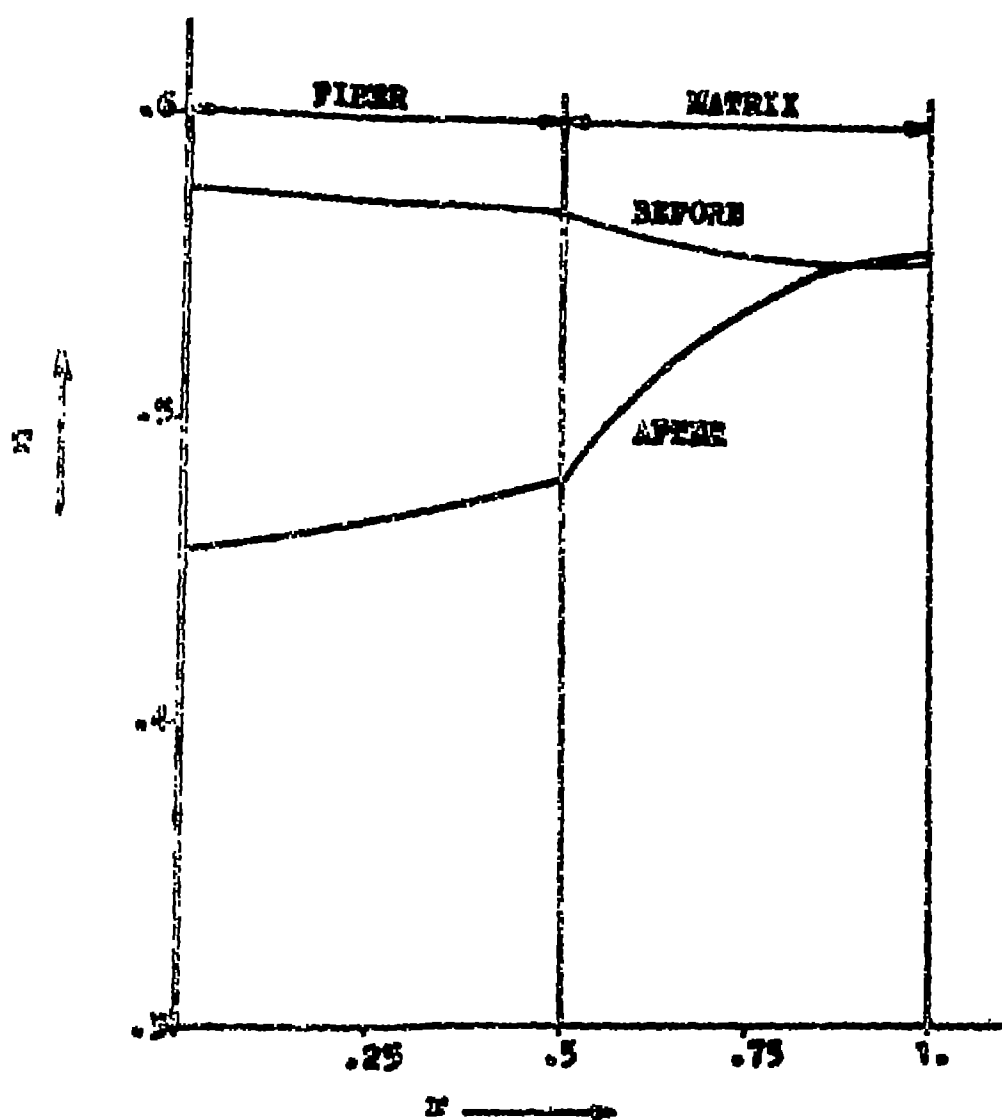


Fig. 3.4 RADIAL TEMPERATURE DISTRIBUTION BEFORE AND
AFTER WITHDRAWAL OF TEMPERATURE SOURCE
(GRAPHITE/EPoxy).

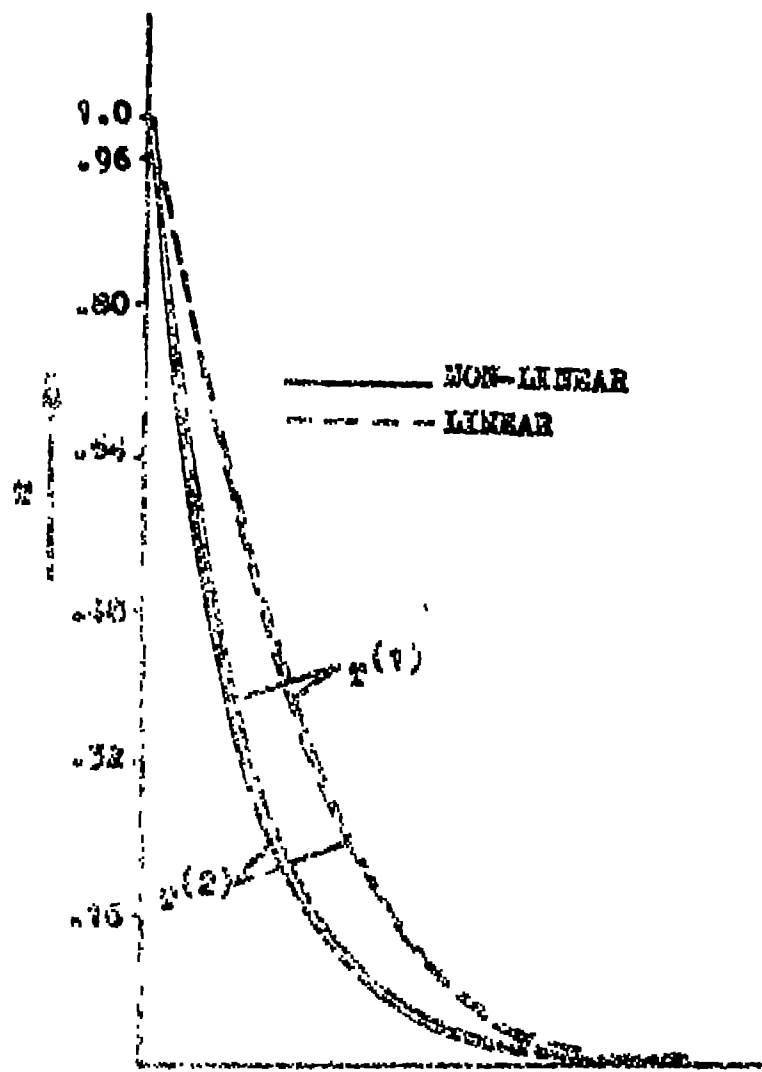


FIG. 3.3 AVERAGE AXIAL TEMPERATURE DISTRIBUTION
WITHOUT REMOVAL OF TEMPERATURE SOURCE
(CHARGE/CHARGE).

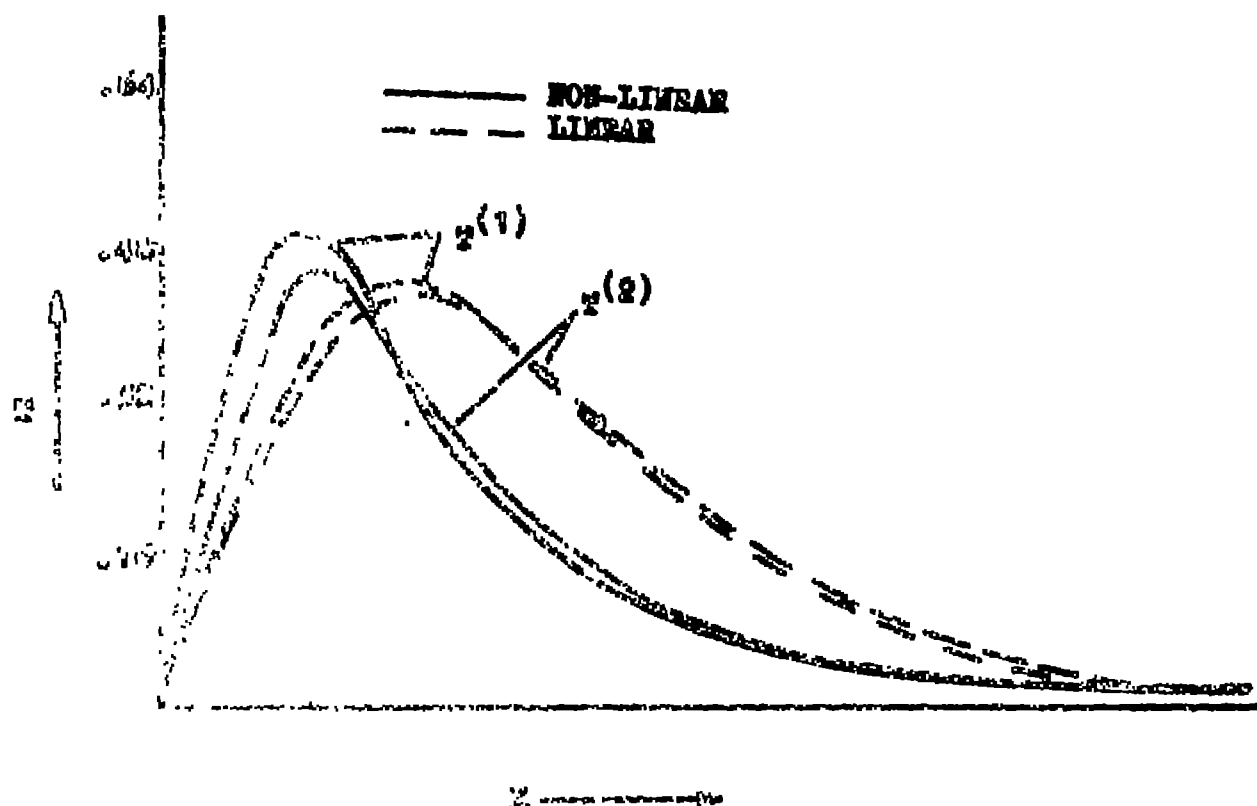


FIG. 5-6 AVERAGE AXIAL TEMPERATURE DISTRIBUTION AFTER
REMOVAL OF TEMPERATURE SOURCE (CARBON/CARBON).

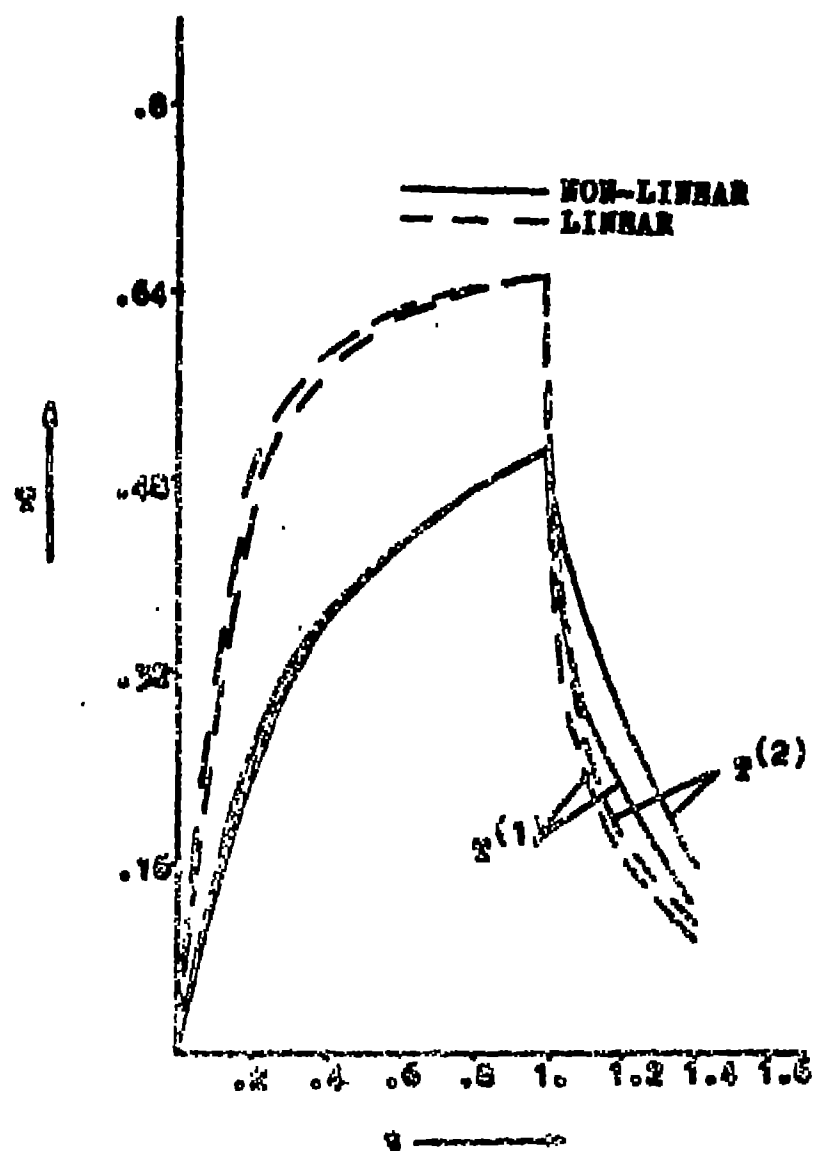


Fig. 3.7 TEMPERATURE TIME HISTORY AT AN
INTERMEDIATE LOCATION (CARBON/CARBON).

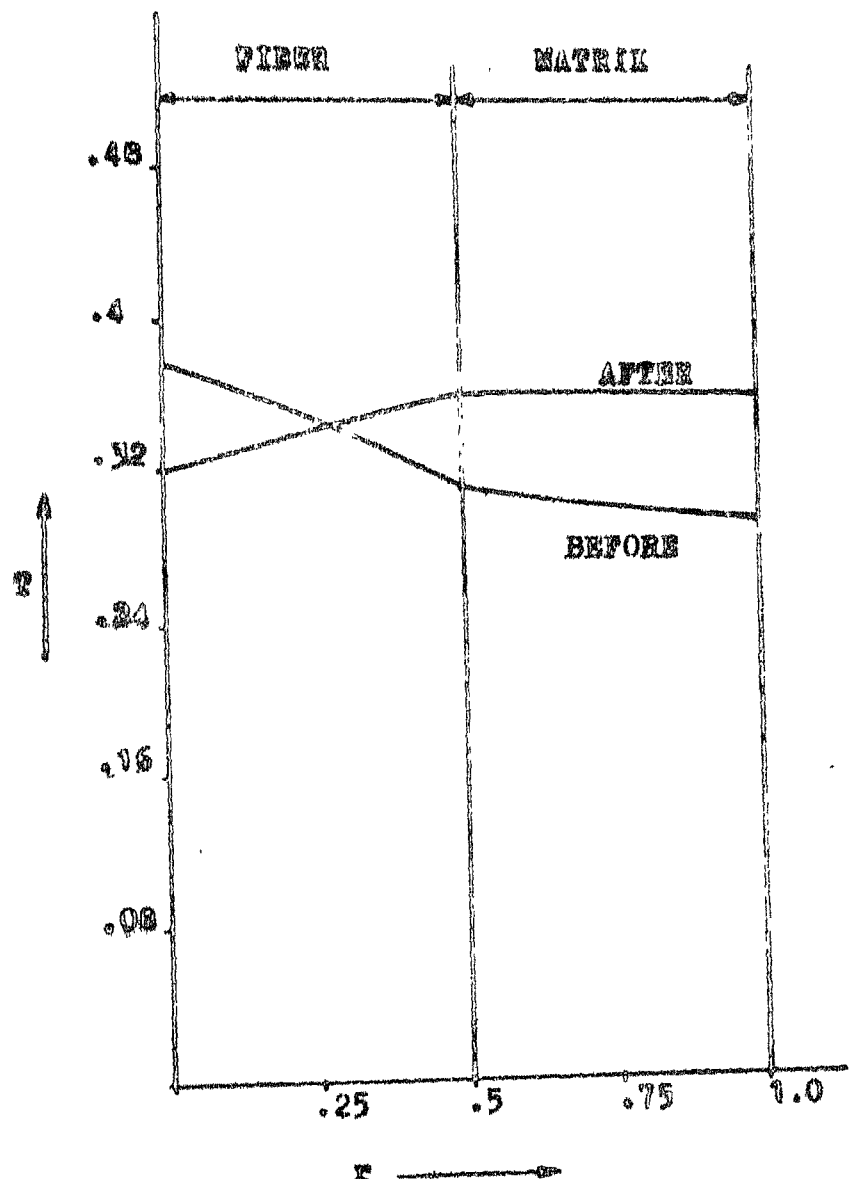


Fig. 3.6 RADIAL TEMPERATURE DISTRIBUTION
BEFORE AND AFTER WITHDRAWAL OF
TEMPERATURE SOURCE (CARBON/CARBON).

REFERENCES

1. Goldstein, H.E., et al., "Opacified silica Reusable Surface Insulation (RSI) for thermal protection of the space shuttle observer", Thermal Conductivity 15, Proceedings of the fifteenth international conference on thermal conductivity held in Ottawa, Ontario, Canada, 1978, Purdue research foundation, Plenum Press PP 353-341.
2. Pierson, H.O., et al., "Carbon felt, carbon matrix composites: Dependence of thermal and mechanical properties on fiber precursor and matrix structure", J. of Composite Materials, Vol. 9, 1975, PP 118-137.
3. Lieberman, M.H., et al., "CVD/PAN felt carbon/carbon composites", J. of Composite Materials, Vol. 9, 1975, PP 337-346.
4. Leelamma, M., et al., "Application of Finite-Element Method of Non-Linear Heat Conduction Problems", Numerical Methods for Coupled Problems, Edited by Hinton E., et al., Pineridge Press, Swansea, U.K., 1981, PP 840-850.

5. Thornton E.A., et al., "Integrated thermal-structural analysis of aerospace structures", Numerical Methods for Coupled Problems, Edited by Hinton E., et al., Pineridge Press, U.K., 1981, PP 817-827.
6. Storm, M.L., J. Applied Physics, Vol. 22, No.7, PP 940-951, July 1951.
7. Pattle, R.E., Quarterly J. Mech. Appl. Math., Vol. 12, PP 407-409, 1959.
8. Yang, K.T., and Szewczyk, A., J. Heat Transfer, PP 251-252, Aug. 1959.
9. Tsang, T., Ind and Eng Chem., Vol. 52, No. 8, PP 707-710, Aug. 1960.
10. Andre-Talaman, T., Int. J. Heat and Mass Transfer, Vol. 11, PP 1351-1357, 1968.
11. Olsson, U., AIAA J., Vol. 8, No. 10, PP 1902-1903, Oct. 1970.
12. Goodman, T.R., Advances in Heat Transfer, Academic Press, Vol.1, PP 51-122, 1964.
13. Imber, M., and Huang, P.N.S., Int. J. Heat and Mass Transfer, Vol. 16, PP 1951-1954, 1973.
14. Pandavan, J., Int. J. Num. Methods in Engg., Vol. 8, PP 295-310, 1974.

15. Bedford, A., and Stern, M., "Towards a diffusing continuum theory of composite materials", *J. Applied Mechanics, Trans. ASME*, PP 3-14, Mar 1971.
16. Stern, M. and Bedford A., "Wave propagation in elastic laminates using a multi-continuum theory", *ACTA Mech.*, Vol. 15, No. 1-2, PP 21-23.
17. Hegemier, G.A., Gurtman, G.A., and Nayfeh, A.H., "A continuum mixture theory of wave propagation in laminated and fibre-reinforced composites", *Int. J. Solids and Structures*, Vol. 9, PP 395-414, 1973.
18. Hegemier, G.A., and Nayfeh, A.H., "A continuum theory for wave propagation in laminated composites: (i) Propagation normal to laminates", *J. Applied Mech.*, Vol. 95, PP 503-510, Jun 1973.
19. Horvay, G., Mani, R., Veluswami, M.A. and Zimsmeister, G.E., "Transient heat conduction in laminated composites", *J. Heat Transfer, Trans. ASME*, Vol. 95, No. 3, PP 309-316, 1973.
20. Padovan, J., "Transient temperature distribution of an anisotropic half space", *AIAA J.*, Vol. 11, PP 565-567, 1973.

21. Padovan, J., "Semi-analytical finite element procedure for conduction in anisotropic axisymmetric solids", *Int. J. Num. Methods in Engg.*, Vol. 8, PP 295-310, 1974.
22. Padovan, J., "Steady conduction of heat in linear and nonlinear fully anisotropic media by Finite Elements", *J. Heat Transfer*, PP 313-318, Aug 1974.
23. Haltman, E.K., Gerrish, R.W. and Krokosky, E.M., "Periodic heat conduction in a 2 phase, 2-D solid domain", *Proc. Int. Heat Transfer Conf.*, 5th, Tokyo, PP 216-219, 1974.
24. Hegemier, G.A. and Bache, T.C., "General continuum theory with microstructure wave propagation in elastic laminated composites", *J. Applied Mech.*, Trans. ASME, Vol. 41, No. 1, PP 97-100, 1974.
25. Hegemier, G.A., "Finite amplitude elastic wave propagation in laminated composites", *J. Applied Physics*, Vol. 45, PP 42-48, 1974.
26. Hegemier, G.A. and Gurtman, G.A., "Finite amplitude elastic-plastic wave propagation fiber-reinforced composites", *J. Applied Physics*, Vol. 45, PP 42-54, 1974.

27. Nayfeh, A.H., "A continuum mixture theory of heat conduction in laminated composites", *J. Appl. Mechanics, Trans. ASME*, Vol. 42, No. 1, PP 165-170, March 1975.
28. Chen, F.C., Choy, C.L. and Young, K., "A theory of thermal conductivity in composite materials", *J. Physics-D (Applied Physics)*, Vol. 9, PP 571-586, 1976.
29. Maewal, A., Bache, T.C. and Hegemier, G.A., "A continuum model for diffusion in laminated composite media", *ASME J. Heat Transfer*, Vol. 98, PP 133-138, 1976.
30. Maewal, A., Gurtman, G.A. and Hegemier, G.A., "A mixture theory for Quasi-One-Dimensional diffusion in fiber reinforced composites", *J. Heat Transfer*, Vol. 100, PP 128-133, 1978.
31. Murakami, H., Hegemier, G.A. and Maewall, A., "A mixture theory for thermal diffusion in unidirectional composites with cylindrical fibers of arbitrary cross-section", *Int. J. Solids and Structures*, Vol. 14, PP 723-737, 1978.
32. Patankar, S.V., "A numerical method for conduction in composite materials, flow in irregular geometries and conjugate heat transfer", *Proc.*

38. Lewis, R.W., Morgan, K., Zienkiewicz, O.C., (Editors), "Numerical Methods in Heat Transfer", John Wiley and Sons Ltd., 1981.
39. Huebner, K.H., "The Finite Element Method for Engineers", A Wiley interscience publication, John Wiley and Sons, Inc., 1980.
40. Necati Ozisik, M., "Heat conduction", A Wiley interscience publication, John Wiley and Sons, Inc., 1980.
41. Hilbert Schenk, Jr., "Fortran Methods in Heat Flow", The Ronald Press Company, 1960.
42. Myers, G., "Analytical Methods in Conduction Heat Transfer", McGraw Hill Book Co., 1971.
43. Rao, S.S. (Editor), "The Finite Element Method", Lectures delivered during the Q.I.P. course held at I.I.T., Kanpur, Department of Mechanical Engineering, I.I.T., Kanpur, March 1975.
44. Zienkiewicz, O.C., Cheung, Y.K., "The Finite Element Method in structural and continuum mechanics", McGraw Hill Book Company, 1968.
45. Segerlind, L.J., "Applied Finite Element Analysis", John Wiley and Sons Inc., 1976.

46. Desai, C.S., Abel, J.F., "Introduction to the Finite Element Method", Lilton Educational Publishing, Inc., Van Nostrand Reinhold Company, New York, 1972.

47. Agarwal, B.D., Broutman, L.J., "Analysis and Performance of Fiber Composites", John Wiley and Sons, Inc., 1980.

APPENDIX 1: PROGRAM LISTING


```

500 90  CONTINUE
500 95  DO 95 I=1,NNODE
500 95  TO(I)=T(I)
500
500 C -----
500 TIME=0.0
500 C -----
500 IR=1 ; M=IB-1 ; M1=IB
500 C -----
500 LOOP FOR INCREMENTS IN TIME
500 DO 500 NIT=1,ITER
500 IF(TIME.LT.TMP) GO TO 106
500 DO 105 K=N+1,NNODE
500 T(K)=0.0
500 105 CONTINUE
500 106 CONTINUE
500 DO 100 I=1,N
500 DO 100 J=1,IB
500 A(I,J)=0.0
500 100 CONTINUE
500 DO 110 I=1,N
500 TO(I)=T(I)
500 T(I)=0.0
500 110 CONTINUE
500 DO 300 IE=1,NELM
500 CALL COND(IE,AE)
500 CALL HTCAP(IE,BE)
500 DO 200 I1=1,3
500 IG=IT(NN(IE,I1))
500 IF(IG.GT.N)GO TO 200
500 DO 200 J1=1,3
500 JG=IT(NN(IE,J1))
500 IF(JG.GT.N)GO TO 150
500 JG1=JG-IG+IB
500 IF(JG1.LE.0 .OR. JG1.GT. IB ) GO TO 145
500 A(IG,JG1)=A(IG,JG1)+AE(I1,J1)+BE(I1,J1)
500 145 CONTINUE
500 T(IG)=T(IG)+(BE(I1,J1)-AE(I1,J1))*TO(JG)
500 GO TO 200
500 150 T(IG)=T(IG)-2.*AE(I1,J1)*TO(JG)
500 200 CONTINUE
500 300 CONTINUE
500 TIME=TIME+DELTA
500 IFAIL=0
500 CALL F04ACF(A,IP4,T,IP1,N,M,IR,T,IP1,A,IP4,M1,IFAIL)
500 IF(IFAIL.EQ.0)GO TO 555
500 WRITE(5,*)IFAIL
500 STOP
500 555 CONTINUE
500 WRITE(51,1007)TIME
500 WRITE(51,1008)(T(IT(I)),I=1,NNODE)
500 500 CONTINUE
500
500 C -----
500 FORMAT STATEMENTS
500 111 FORMAT(1H , 'INCREASE IP1')
500 112 FORMAT(1H , 'INCREASE IP2')
500 113 FORMAT(1H , 'INCREASE IP3')
500 114 FORMAT(1H , 'INCREASE IB1 TO ',I2)
500 1000 FORMAT(20A4)
500 1001 FORMAT(1H , '20A4')
500 1002 FORMAT(1H , 'NUMBER OF NODES= ',I3,'/1H , 'NUMBER OF ELEMENTS=',
500 113,'/1H , 'NUMBER OF MATERIALS= ',I2,'/1H , 'INCREMENTAL TIME=',
500 121,'/1H , 'NO. OF NODES WITH SPECIFIED TEMPS= ',I3,'/1H , 'NO.
500 122,'/1H , 'NO. OF NODES WITH SPECIFIED TEMPS= ',I3,'/1H , 'NO.
500 1003 FORMAT(1H , '20X , 'NODAL INFORMATION'//1H ,8X , 'NODE',15X,
500 1004 FORMAT(1H , '20X , 'CORD' ,10X , 'T' ,//)
500 1005 FORMAT(6X , 'NODE' ,I3 ,5X ,3E15.5//)
500 1006 FORMAT(1H , '20X , 'ELEMENT INFORMATION'//1H ,7X , 'ELE' ,3X , 'I',
500 115,'/5X , 'K' ,3X , 'MATERIAL'//)
500 1007 FORMAT(6X ,I3 ,3I6 ,4X ,I4)
500 1008 FORMAT(1H , 'TIME= ',F11.5)
500 1008 FORMAT(5(1PE16.4))
500 550 CLOSE(UNIT=50)
500 560 CLOSE(UNIT=51)
500 570 END
500
500 C -----
500 590 C -----
500 600 C -----
500 600 SUBROUTINE TO CALCULATE ELEMENTAL CONDUCTIVITY MATRIX.
500 610 C -----
500 620 C -----
500 620 SUBROUTINE COND(N,AE)
500 630 C -----
500 630 PARAMETER IP1=80,IP2=120
500 630 COMMON NN(IP2,3),XCORD(IP1),YCORD(IP1),MATL(IP2),DELTA,TO(IP1)
500 640 C -----
500 640 1,IT(IP1)
500 650 C -----
500 650 DIMENSION AE(3,3)
500 660 C -----
500 660 FIND THE NODE NUMBERS OF THE ELEMENT
500 670 C -----
500 670 I=NN(N,1)

```


200
300
400
500
600
700
800
900
000
100
200
300
400
500
600
700 91 1TAV/1000.)**3)-0.0412*((TAV/1000.)**4)
CONTINUE
COEFF=HC*AREA/60.
FACT=2./DELTA
REC(1,1)=COEFF*EL11*FACT
REC(1,2)=COEFF*EL12*FACT
REC(1,3)=COEFF*EL13*FACT
REC(2,2)=COEFF*EL22*FACT
REC(2,3)=COEFF*EL23*FACT
REC(3,3)=COEFF*EL33*FACT
REC(2,1)=REC(1,2)
REC(3,1)=REC(1,3)
REC(3,2)=REC(2,3)
RETURN
END
C

APPENDIX 2

Material properties for Graphite/Epoxy composite

	Axial Thermal Conductivity $K_{xx}^{(\alpha)}$	Radial Thermal Conductivity $K_{rr}^{(\alpha)}$	Heat capacity $\mu^{(\alpha)}$
Fiber $(\alpha=1)$	$K_{xx}^{(1)} = 10 - 0.01 T^{(1)}$	$K_{rr}^{(1)} = 8 - 0.008 T^{(1)}$	$\mu^{(1)} = 0.875 + 0.004 T^{(1)}$ $- 5 \times 10^{-6} (T^{(1)})^2$
Matrix $(\alpha=2)$	$K_{xx}^{(2)} = 1 + 0.005 T^{(2)}$	$K_{rr}^{(2)} = 1 + 0.005 T^{(2)}$	$\mu^{(2)} = 1 + 0.002 T^{(2)}$ $+ 1.5 \times 10^{-6} (T^{(2)})^2$

APPENDIX 3

Material properties of carbon/carbon composite

	a_0	a_1	a_2	a_3	a_4
$K_{xx}^{(1)}$	1069.42	- 1119.78	646.40	- 179.327	19.1263
$K_{xx}^{(2)}$	178.20	- 31.678	6.015	0	0
$K_{rr}^{(1)}$	110.84	- 106.12	54.24	- 13.52	1.1647
$K_{rr}^{(2)}$	178.20	- 31.678	6.015	0	0
$\mu^{(1)}$	0.2937	1.0962	- 0.3448	0.3129	-0.0436
$\mu^{(2)}$	0.2776	1.0361	- 0.7984	0.2953	-0.0412

Note : $[K_{xx}^{(\alpha)}] = [K_{rr}^{(\alpha)}] = \text{cal/cm-hr-}^{\circ}\text{C}$

$[\mu^{(\alpha)}] = \text{cal/cm}^3\text{-}^{\circ}\text{C}$

A 83400

ME-1984-M-SOM-FIN